Editors' Suggestion

Nonequilibrium turbulent dissipation in buoyant axisymmetric plume

Sunita [*] and G. C. Layek [†]

Department of Mathematics, The University of Burdwan, Burdwan-713104, West Bengal, India

(Received 10 June 2021; accepted 27 August 2021; published 8 October 2021)

We report existence of nonequilibrium turbulent dissipations in buoyant axisymmetric plumes at infinite Reynolds number limit. The plume statistical equations remain form invariant under one translation parameterized by a_0 and two unequal stretching transformations parameterized by a_1 and a_2 of flow variables, except the pressure-strain-rate equation. The dissipation coefficients, unlike Kolmogorov theory, in the scaling of dissipations ϵ_u of velocity fluctuation u' and ϵ_θ of thermal fluctuation θ' evolve linearly with spreading rate $d\delta/dz$. The spreading rate is expressed as inversely proportional to local Reynolds number Re_δ raised to the exponent $m = 3(a_1 - a_2)/(a_1 + a_2)$, $a_1 \neq -a_2$ and is varying with Re_δ for $m \neq 0$. The components of Reynolds stress tensor have different streamwise (s) evolutions as $(\overline{w'^2})_s = (\overline{v'^2})_s \propto (d\delta/dz)^2(\overline{u'^2})_s$ and $(\overline{u'v'})_s \propto d\delta/dz(\overline{u'^2})_s$ unless $d\delta/dz$ is a constant, which holds only if $m = 0$ giving $a_1 = a_2$. This implies that Kolmogorov equilibrium theory ($m = 0$) is intertwined inextricably with complete self-preservation. There is a direct universal relationship between turbulent dissipation and entrainment coefficient α as $d\delta/dz \propto \alpha$, the proportionality constant depends on integrals of mean axial velocity, temperature difference, and turbulent stresses. The power exponent in power-law streamwise evolutions of flow quantities are specified by the ratio a_2/a_1 and differs from the conventional results unless $m = 0$. Both the local axial velocity and temperature difference widths are increasing with the increase of vertical distance from the source, as same power-law scaling exponents but differ due to different prefactors. However, the spreading rates and entrainment coefficient decrease in the non-Kolmogorov dissipation region, which occurs when $m \neq 0$ preferably lying in (0,1] ($a_2/a_1 \in [1/2, 1)$). Similar trends of spreading rate and entrainment were also measured experimentally in planar jet [Cafiero and Vassilicos, Proc. R. Soc. London A **475**, 20190038 (2019)] and established theoretically in planar jet and plume [Layek and Sunita, Phys. Rev. Fluids **3**, 124605 (2018); Layek and Sunita, Phys. Fluids **30**, 115105 (2018)].

DOI: 10.1103/PhysRevFluids.6.104602

I. INTRODUCTION

Turbulent plumes are ubiquitous in nature and industries. Plumes are generated under gravity due to the density (temperature) differences between the source fluid and the fluid in the ambient environment, and spread by entraining the nonturbulent ambient fluid into the plume. The buoyancy force causes the plume to deflect vertically against gravity when the ambient environment is stagnant and is heavier than the plume. The density or temperature of the ambient can be either constant, called an unstratified (neutral) environment, or can vary with the vertical distance, called a stratified environment. Here we study turbulent round (axisymmetric) buoyant plume in neutral ambient. So the plume is generated by a pure buoyancy source where the buoyancy flux is a constant at the source

[*] sunitanayak1989@gmail.com

[†] gclayek@math.buruniv.ac.in

and is conserved as the plume elevates, that is, vertical gradient of buoyancy flux vanishes. The source Richardson's number $\mathrm{Ri}_0 \approx 1$ or the volume and momentum fluxes are zero at the source and increase as the plume rises upwards. The plume velocity and the active temperature fields interact with each other, which results in the turbulent kinetic energy (TKE) production (see Refs. [1–3]).

Since the earliest work of Zel'dovich [4] followed by Schmidt [5] on free convection turbulent flows, researchers primarily focused on the self-similar behavior of turbulent plumes at different vertical stations far away from the source. Batchelor [1] in his partial theoretical analysis and Rouse *et al.* [6] obtained solutions of both the planar and the axisymmetric turbulent plumes by considering them to be of self-preserving nature separable into a scaling function and a self-preserving profile function. Further, the scaling functions were assumed beforehand as power laws of streamwise distance independent of cross-stream variations. On dimensional grounds the exact values of the power exponent were determined from the model equations. However, even now determining the profile functions, which depend on a new independent variable called as similarity variable is very difficult analytically, particularly for higher-order correlations due to the closure problem. Yih [7] obtained the forms of the self-preserving profile functions of mean velocity and mean temperature difference, but that too only for some special cases. Another approach is the modified equilibrium similarity hypothesis by George [8] in which although the solutions are assumed to be separable and self-preserving as discussed above, but the form of scaling function is not predicted *a priori*. The scaling relations are set up keeping the equations self-similar. These relations with some assumptions on spreading rate and dissipation laws provide the desired scaling laws [8,9]. However, whatever the approach, the assumption of Kolmogorov equilibrium similarity hypothesis in the inertial range of turbulence is the cornerstone assumption in obtaining the conventional power-law scalings and the self-preserving functions. According to the Kolmogorov equilibrium similarity hypothesis in the inertial range, dissipations of turbulent kinetic energy $\overline{k}$ and turbulent thermal intensity $\overline{k_\theta}$ obey the laws $\epsilon = C_\epsilon(\overline{k})^{3/2}/\delta$ and $\epsilon_\theta = C_{\epsilon_\theta}(\overline{k})^{1/2}\overline{k_\theta}/\delta$, where δ is the local width of the flow and the dissipation coefficients C_ϵ and C_{ϵ_θ} are constants of order unity and may vary from one flow to another.

The significance of Kolmogorov similarity hypothesis is that complete self-preservation holds in the region specified. By complete self-preservation we mean that all the averaged equations, Reynolds stress balance equations, turbulent kinetic energy equation, pressure-strain-rate equation (which appears due to the continuity equation) maintain self-similarity. This also indicates that the components of Reynolds stress tensor scale in the same way with the streamwise distance above the virtual origin as the turbulent kinetic energy, i.e., $(\overline{u'^2})_s \sim (\overline{v'^2})_s \sim (\overline{w'^2})_s \sim (\overline{u'v'})_s \sim (\overline{k})_s$. Further, the dissipations of normal stress tensor ϵ_u, ϵ_v, and ϵ_w scale in the same way as the dissipation of turbulent kinetic energy ϵ. At the centerline, $\epsilon_u = \epsilon_v = \epsilon_w = 2\epsilon/3$ and the dissipation of Reynolds shear stress $\epsilon_{uv} = 0$.

The conventional scaling laws of the centerline axial velocity $\overline{u}_c$ and the centerline mean temperature (density) difference θ_c of the unstratified axisymmetric plume were obtained as $\overline{u}_c \propto z^{-1/3}$ and $g\beta\theta_c \propto z^{-5/3}$, β is constant thermal expansion coefficient. Also, the plume spreading rates were found to remain constant with increasing vertical height z of the plume. The unstratified plumes generated in the laboratory by different experimental techniques (see Refs. [2,5,6,10–12]) verified the power-law forms of the scaling functions and that the profiles functions are self-preserving far from boundaries. However, the spreading rates of plumes for different experiments are not found same (see Refs. [2,6,12]), so it is inferred that the scaling laws might depend on source conditions. This is in contrast to the classical equilibrium similarity hypothesis for free shear turbulent flows by Townsend [13], but agrees with the modified hypothesis by George [8]. Nevertheless, the differences are sometimes attributed to the limitations in experimental setups and errors in measurements [14].

The entrainment assumption pioneered by Taylor [15] (see Refs. [14,16–18]) is another widely used approach to study various kinds of plumes. In this approach, it was assumed that the radial velocity at the edge of the steady plume is directly proportional to the axial velocity. The proportionality constant is the entrainment parameter, which lacks uniqueness for different experiments.

This approach also reported the conventional scaling laws of centerline velocity, active scalar, and plume widths using complete similarity hypothesis of Kolmogorov. It is shown first time in Layek and Sunita [19] that conventional scaling laws and constant entrainment coefficient can occur in planar plume if and only if turbulent dissipations obey Kolmogorov equilibrium law. Otherwise, for non-Kolmogorov dissipations the entrainment parameter can vary with the streamwise distance. Based on a model on entrainment assumption, Lane-Serff [20] mentioned that in jets and plumes the energy dissipation is $\epsilon = \alpha U^3/R$ where U is mean centerline speed, R is radius of plume/jet, and α is the entrainment constant, which is different for plumes and jets. The dissipation rate would differ in general if the entrainment constant differed in different circumstances. The recent theoretical and experimental studies [19,21,22] on the existence of non-Kolmogorov turbulence dissipation implied that this direct link between entrainment and dissipation may hold in general irrespective of the scaling law followed by turbulent energy dissipation.

It is well known that Kolmogorov theory maintains complete self-similarity for isotropic inertial range turbulence. However, there exist measurements which showed that components of a flow variable scale in different ways, and these scalings are physically relevant. So, Kolmogorov theory has limitations although it has had great impact. Researchers are continually exploring what lies beyond Kolmogorov. The theoretical and experimental studies [8,9,19,21,22] showed that turbulent dissipations would follow the Kolmogorov equilibrium laws in jets and plumes only if the spreading rates do not vary with the streamwise distance. However, Kotsovinos [23] and later Bradshaw [24] found an increase in the spreading rate of turbulent jet with increase in streamwise distance. It is suggested that this may not support the Kolmogorov's theory of equilibrium dissipation (see Ref. [21]).

Layek and Sunita [19,21,25] found self-similar behavior of statistical equations subject to invariance of the conserved quantity in jets, wakes, and plumes even when complete self-preservation does not hold, called the partial or incomplete self-similarity. In this situation, the dissipation laws occur with nonconstant dissipation coefficient $C_\epsilon \propto d\delta/dz$. In a particular case when local Reynolds number $\mathrm{Re}_\delta(=\bar{k}_s^{1/2}\delta/\nu$, $\bar{k}$ is mean TKE) is not a constant but varies with streamwise distance, then $C_\epsilon \propto (\mathrm{Re}_G/\mathrm{Re}_\delta)^m$ with $m \neq 0$, where $\mathrm{Re}_G = (u_0 z_0/\nu)$ is the global/inlet Reynolds number, subscript "0" indicates flow velocity and width at the source. It implies that in this case the spreading rate $d\delta/dz \propto (\mathrm{Re}_G/\mathrm{Re}_\delta)^m$ and is valid only for a range of values of m. This particular distinction of dissipation coefficient C_ϵ is observed experimentally and found by the direct numerical simulations (DNS) (Refs. [22,26,27]), particularly and most preferably for $m = 1$, and is also established theoretically [19,21,25]. Nedic *et al.* [26] recorded the non-Kolmogorov scaling in axisymmetric wake for a very long distance from the source, that is about 50 times the square root of wake source area. Caifero and Vassilicos obtained this non-Kolmogorov scaling experimentally in planar jet in a region downstream of $x \approx 20h$ to $x \approx 140h$, h is the size of the nozzle exit section.

However, although the statements of the non-Kolmogorov dissipation laws are the same in Refs. [22,27] and Layek and Sunita [21,25], the scaling laws of the statistical quantities differ in these works for $m \neq 0$ and $m \neq 1$. The differences are primarily due to different scaling of turbulent kinetic energy for $m \neq 0$. Note that Refs. [19,21] found $\bar{k}_s = \bar{u}_s^2$, while Cafiero and Vassilicos [22] found $\bar{k}_s = \bar{u}_s^2 d\delta/dx$. However, Layek and Sunita [19,21] stressed the preference of $C_\epsilon \propto d\delta/dx$ over $\propto (\mathrm{Re}_G/\mathrm{Re}_\delta)^m$, as it would include the turbulent flows where local Reynolds number is not varying with streamwise distance.

The varying nature of dissipation coefficient and its dependence on source conditions in various turbulent flows provide substantial evidence of nonuniversality of turbulent energy dissipation (see also Refs. [28–30]). Here Lumley's [31] remark on the nongenerality of Kolmogorov laws for turbulent dissipations and his emphasis on their remodelling are worth mentioning. Lumley's premonition about the abandonment of Kolmogorov law for passive scalar dissipation in case of failure of the law for energy dissipation is found to be true and established theoretically by Layek and Sunita [19], where the dissipation of turbulent scalar (thermal) fluctuation, which is an active contaminant in plume, obeys non-Kolmogorov law in the regimes where turbulent energy

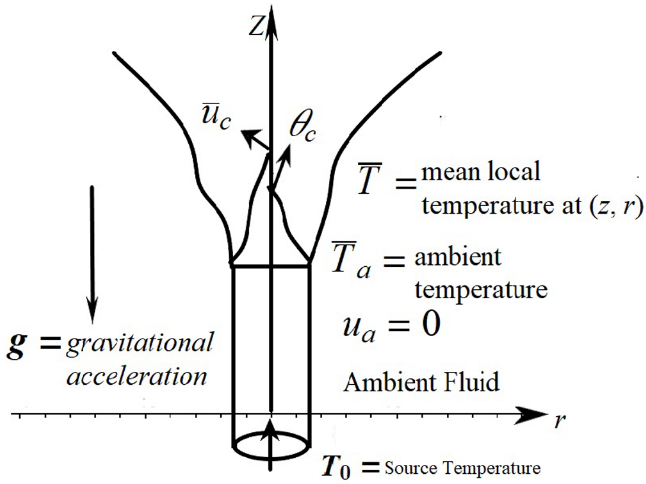

FIG. 1. Axisymmetric plume flow definition.

dissipation is non-Kolmogorov so that both C_ϵ and C_{ϵ_θ} vary with the local Reynolds number as $C_\epsilon \propto (\mathrm{Re}_G/\mathrm{Re}_\delta)^m \propto C_{\epsilon_\theta}$ with $m \neq 0$. In general this is true when $C_\epsilon \propto d\delta/dz \propto C_{\epsilon_\theta}$.

The essence of this work is to establish the relation between the dissipation and spreading rate in axisymmetric plume, which in other way, provides a link between entrainment and dissipation representing both Kolmogorov and non-Kolmogorov regions of turbulent dissipations. The dissipation distinction appears due to different axial evolutions of components of Reynolds stress tensor, pressure-strain-rate tensor, etc., giving an incomplete/partial self-similarity of incompressible pressure-strain-rate equation. The main implications of nonequilibrium scaling are due to the change of streamwise scaling exponents. It is shown that the classical turbulence closure models are not valid in the non-Kolmogorov region. Symmetry-based eddy viscosity closure is designed to explore the profiles in non-Kolmogorov regions.

II. FLOW DESCRIPTION OF TURBULENT ROUND BUOYANT PLUME

Consider a steady axisymmetric plume with no swirl, which is formed due to the difference in local mean temperature of a stream of fluid at temperature T_0 (reference temperature) issued through a circular source into a quiescent ambient and T_a is the constant temperature of the ambient. The axial distance z is vertical opposite to the direction of gravitational acceleration g, and r is the radial direction perpendicular to the direction of plume source. The prime of a variable denotes turbulent fluctuation and a bar over a variable denotes its average. Here the initial Richardson number $\mathrm{Ri}_0 \approx 1$, so the flow is a plume from the outset (see Refs. [10,12]). The local mean axial velocity $\overline{u}$ is in the vertical direction z, $\overline{v}$ is the mean cross-stream velocity, which is in radial direction r, $\overline{w}$ is the mean velocity in the azimuthal direction φ and $\overline{T}$ is the local mean temperature. The velocity fluctuations u', v', and w' are in z, r, and φ directions, respectively, p' is the pressure fluctuation and θ' is the temperature fluctuation. Due to axisymmetry, the flow variables are dependent only on z and r coordinates and hence $\partial/\partial\varphi = 0$. For no swirl $\overline{w} = 0$, $\overline{u'w'} = 0$, and $\overline{v'w'} = 0$. A sketch of the axisymmetric plume is given in Fig. 1.

The mean continuity, mean momentum, and mean temperature difference equations of the steady axisymmetric plume with zero free stream pressure gradient, boundary layer approximations, and Boussinesq assumption for natural convection with constant ambient temperature denoted by T_a are expressed by [2]

$$\frac{\partial \bar{u}}{\partial z} + \frac{1}{r}\frac{\partial (r\bar{v})}{\partial r} = 0, \tag{1a}$$

$$\bar{u}\frac{\partial \bar{u}}{\partial z} + \bar{v}\frac{\partial \bar{u}}{\partial r} = g\beta\theta - \frac{1}{r}\frac{\partial (r\overline{u'v'})}{\partial r} - \frac{\partial (\overline{u'^2} - \overline{v'^2})}{\partial z} + \frac{\nu}{r}\frac{\partial}{\partial r}\left(r\frac{\partial \bar{u}}{\partial r}\right), \tag{1b}$$

$$\bar{u}\frac{\partial \theta}{\partial z} + \bar{v}\frac{\partial \theta}{\partial r} = -\frac{\partial \overline{u'\theta'}}{\partial z} - \frac{1}{r}\frac{\partial (r\overline{v'\theta'})}{\partial r} + \kappa\frac{\partial}{\partial r}\left(r\frac{\partial \theta}{\partial r}\right). \tag{1c}$$

Here $\beta\theta(z, r) = \beta[\overline{T}(z, r) - T_a] = [\rho_a - \rho(z, r)]/\rho_0 \ll 1$, where $\beta = 1/T_0$ is the coefficient of thermal expansion and is considered as constant, $\rho(z, r)$ is the local mean density, ρ_a is the constant ambient density, and ρ_0 the reference density. $\overline{u'\theta'}$ and $\overline{v'\theta'}$ are turbulent heat fluxes in the axial and radial directions, respectively, and $\overline{u'v'}$ is the Reynolds shear stress. Due to the Boussinesq approximation, the temperature (density) appears in the mean momentum equation only when multiplied by the acceleration due to gravity g. The terms multiplied by the kinematic fluid viscosity ν and the thermal diffusivity $\kappa = \nu/\sigma$, where σ the molecular Prandtl number are viscous and molecular thermal dissipation, respectively. At high enough Reynolds number these terms in the equations can be neglected. The term involving $(\overline{u'^2} - \overline{v'^2})$ in Eq. (1b) and the diffusion due to the axial turbulent heat flux $\overline{u'\theta'}$ in Eq. (1c) are found to be very small under traditional analysis and boundary layer approximations and they are therefore usually neglected.

The boundary conditions are

$$\bar{u} = \bar{u}_c,\ \frac{\partial \bar{u}}{\partial r} = 0,\ \theta = \theta_c,\ \frac{\partial \theta}{\partial r} = 0,\ \overline{u'v'} = 0,\ \overline{v'\theta'} = 0 \text{ at } r = 0, \tag{2a}$$

$$\bar{u} = 0,\ \frac{\partial \bar{u}}{\partial r} = 0,\ \theta = 0,\ \frac{\partial \theta}{\partial r} = 0,\ \overline{u'v'} = 0,\ \overline{v'\theta'} = 0,\ \text{at } r = \pm\infty. \tag{2b}$$

The Reynolds stress model under boundary layer and Boussinesq approximations (see Ref. [2]) is given by

$$\bar{u}\frac{\partial \overline{u'^2}}{\partial z} + \bar{v}\frac{\partial \overline{u'^2}}{\partial r} = -\frac{1}{r}\frac{\partial (r\overline{u'^2v'})}{\partial r} - 2\overline{u'v'}\frac{\partial \bar{u}}{\partial r} - 2\overline{u'^2}\frac{\partial \bar{u}}{\partial z} + 2g\beta\overline{u'\theta'} + 2p_u - \frac{2}{\rho_0}\frac{\partial \overline{p'u'}}{\partial z} + \frac{\nu}{r}\frac{\partial}{\partial r}\left(r\frac{\partial \overline{u'^2}}{\partial r}\right) - 2\epsilon_u, \tag{3a}$$

$$\bar{u}\frac{\partial \overline{v'^2}}{\partial z} + \bar{v}\frac{\partial \overline{v'^2}}{\partial r} = -\frac{1}{r}\frac{\partial r\overline{v'^3}}{\partial r} + 2\frac{\overline{w'^2v'}}{r} - 2\overline{v'^2}\frac{\partial \bar{v}}{\partial r} - 2P_v + \frac{\nu}{r}\frac{\partial}{\partial r}\left(r\frac{\partial \overline{v'^2}}{\partial r}\right) - 2\epsilon_v; \tag{3b}$$

$$\bar{u}\frac{\partial \overline{w'^2}}{\partial z} + \bar{v}\frac{\partial \overline{w'^2}}{\partial r} = -\frac{1}{r}\frac{\partial (r\overline{w'^2v'})}{\partial r} - 2\frac{\overline{w'^2v'}}{r} - 2P_w - 2\frac{\bar{v}}{r}\overline{w'^2} + \frac{\nu}{r}\frac{\partial}{\partial r}\left(r\frac{\partial \overline{w'^2}}{\partial r}\right) - 2\epsilon_w, \tag{3c}$$

$$\bar{u}\frac{\partial \overline{u'v'}}{\partial z} + \bar{v}\frac{\partial \overline{u'v'}}{\partial r} = -\overline{v'^2}\frac{\partial \bar{u}}{\partial r} - \overline{u'v'}\frac{\partial \bar{v}}{\partial r} + \frac{\overline{u'w'^2}}{r} - \frac{1}{r}\frac{\partial (r\overline{u'v'^2})}{\partial r} + p_{uv} - \frac{1}{\rho_0}\left(\frac{\partial \overline{p'u'}}{\partial r} + \frac{\partial \overline{p'v'}}{\partial z}\right) + \frac{\nu}{r}\frac{\partial}{\partial r}\left(r\frac{\partial \overline{u'v'}}{\partial r}\right) - 2\epsilon_{uv}. \tag{3d}$$

The terms $\overline{u'^2}$, $\overline{v'^2}$, and $\overline{w'^2}$ are the Reynolds normal stresses in the z, r, and φ directions, respectively. The terms involving kinematic viscosity ν denote viscous diffusions and are neglected at the infinite-Reynolds-number limit; ϵ_u, ϵ_v, ϵ_w, and ϵ_{uv} are the components of homogeneous-dissipation; the gradients of triple velocity correlations $\overline{u'^2v'}$, $\overline{u'w'^2}$, $\overline{v'^3}$, and $\overline{w'^2v'}$ denote turbulent diffusions, $p_u = \overline{\frac{p'}{\rho_0}\frac{\partial u'}{\partial z}}$, $p_v = \overline{\frac{p'}{\rho_0}\frac{\partial v'}{\partial r}}$, $p_w = \overline{\frac{p'}{\rho_0}(\frac{1}{r}\frac{\partial w'}{\partial \varphi} + \frac{v'}{r})}$, and $p_{uv} = \overline{\frac{p'}{\rho_0}(\frac{\partial u'}{\partial r} + \frac{\partial v'}{\partial z})}$ are the pressure-strain-rate terms. Here the velocity-pressure gradients $P_v = \overline{\frac{v'}{\rho_0}\frac{\partial p'}{\partial r}} = \frac{1}{\rho_0}\frac{\partial \overline{p'v'}}{\partial r} - p_v$ and $P_w = \frac{1}{\rho_0}\overline{\frac{w'}{r}\frac{\partial p'}{\partial \varphi}} = \frac{1}{\rho_0 r}(\frac{\partial \overline{p'w'}}{\partial \varphi} + \overline{p'v'}) - p_w$. Note that $\frac{\partial \overline{p'w'}}{\partial \varphi} = 0$ because of axial symmetry of the plume.

The mean balance equation for the intensity of temperature fluctuations under boundary layer approximations is given by

$$\overline{u}\frac{\partial \overline{k_\theta}}{\partial z} + \overline{v}\frac{\partial \overline{k_\theta}}{\partial r} = \frac{\kappa}{r}\frac{\partial}{\partial r}\left(r\frac{\partial \overline{k_\theta}}{\partial r}\right) - \frac{1}{r}\frac{\partial r\overline{v'k_\theta}}{\partial r} - \overline{u'\theta'}\frac{\partial \theta}{\partial z} - \overline{v'\theta'}\frac{\partial \theta}{\partial r} - \epsilon_\theta, \tag{4}$$

where $\overline{k_\theta}$ with $k_\theta = \theta'^2/2$ is the mean of the intensity of temperature fluctuation θ' and ϵ_θ is the dissipation of $\overline{k_\theta}$. The first term in right-hand side of Eq. (4) involving κ is the molecular thermal diffusion.

The turbulent kinetic energy equation under boundary layer and Boussinesq approximations is given by

$$\overline{u}\frac{\partial \overline{k}}{\partial z} + \overline{v}\frac{\partial \overline{k}}{\partial r} = \frac{\nu}{r}\frac{\partial}{\partial r}\left(r\frac{\partial \overline{k}}{\partial r}\right) - \frac{1}{r}\frac{\partial(r\overline{v'k + p'v'/\rho_0})}{\partial r} - \overline{u'v'}\frac{\partial \overline{u}}{\partial r} - (\overline{u'^2} - \overline{v'^2})\frac{\partial \overline{u}}{\partial z} + \beta g\overline{u'\theta'} - \epsilon. \tag{5}$$

The integral form of the mean continuity Eq. (1a), mean momentum Eq. (1b), and mean temperature difference Eq. (1c) multiplied by $g\beta$ are obtained as

$$\frac{d}{dz}Q(z) = -[r\overline{v}(z,r)]_0^\infty, \tag{6a}$$

$$\frac{d}{dz}M(z) = \int_0^\infty g\beta\theta r dr, \tag{6b}$$

$$\frac{d}{dz}B_F(z) = 0, \tag{6c}$$

where $Q(z)$ is the kinematic volume flux, $M(z)$ is the kinematic momentum flux, and $B_F(z)$ is the kinematic buoyancy flux and are given by

$$Q(z) = 2\pi\int_0^\infty \overline{u} r dr, \tag{7a}$$

$$M(z) = M_m + M_f = 2\pi\int_0^\infty \overline{u}^2 r dr + 2\pi\int_0^\infty (\overline{u'^2} - \overline{v'^2}) r dr, \tag{7b}$$

$$B_F(z) = B_{F_m} + B_{F_f} = 2\pi\int_0^\infty g\beta\theta\overline{u} r dr + 2\pi\int_0^\infty g\beta\overline{u'\theta'} r dr. \tag{7c}$$

Here $M_m = 2\pi\int_0^\infty \overline{u}^2 r dr$, $M_f = 2\pi\int_0^\infty (\overline{u'^2} - \overline{v'^2}) r dr$, $B_{F_m} = 2\pi\int_0^\infty g\beta\theta\overline{u} r dr$, and $B_{F_f} = 2\pi\int_0^\infty g\beta\overline{u'\theta'} r dr$. Note that since the ambient temperature T_a is a constant, the square of the local buoyancy frequency N^2 given by $N^2 = g\beta\frac{dT_a(z)}{dz}$ is zero and B_F is a constant in z equal to the buoyancy flux at the source of the plume B_{F0}(say). Note that if T_a was not a constant but varied as a function of z, then B_F and N^2 would have been varied with z. Here we shall discuss the scaling laws for plume in unstratified ambient only at the infinite-Reynolds-number limit.

III. ANALYSIS

We adopt Lie symmetry analysis which delivers self-similar solutions under which the above statistical equations remain invariant. Note that Layek and Sunita [19] predicted theoretically by adopting Lie symmetry group theory on the statistical turbulent model equations of a planar turbulent pure plume that dissipations of turbulent kinetic energy and turbulent thermal fluctuation, and entrainment coefficients are different from Kolmogorov and called as non-Kolmogorov. Here we extend the same sort of analysis to turbulent round buoyant plume in unstratified stagnant ambient for identifications of new scaling laws, spreading rate, and dissipation laws. However, instead of considering only the budget equation of turbulent kinetic energy and equation of intensity of thermal fluctuation, we have considered in addition the budget equation of individual Reynolds stresses, also called as Reynolds stress model. The Reynolds stress model is necessary as one can determine the scaling of individual Reynolds stress components and pressure-strain-rate components and their contributions in turbulence dynamics.

A. Symmetry analysis of statistical equations

Lie symmetry group theory is well documented in standard books [32]. Here we found the scaling laws of the flow variables with the increase in vertical distance by the symmetry analysis of Reynolds stress model, turbulent kinetic energy equation, thermal fluctuation equation along with the mean continuity, mean momentum, and mean temperature difference equations with zero free stream pressure gradient. Some experimental measurements found the role of pressure-strain-rate terms in the redistribution of energy by assuming the terms $\frac{1}{\rho_0}\frac{\partial\overline{p'u'}}{\partial z}$ and $\frac{1}{\rho_0}(\frac{\partial\overline{p'u'}}{\partial r}+\frac{\partial\overline{p'v'}}{\partial z})$ negligible in comparison to the pressure-strain-rate terms (see the work of Hussein *et al.* [33] for axisymmetric jet). Here we assume that $\frac{1}{\rho_0}\frac{\partial\overline{p'u'}}{\partial z} \ll p_u$ and $\frac{1}{\rho_0}(\frac{\partial\overline{p'u'}}{\partial r}+\frac{\partial\overline{p'v'}}{\partial z}) \ll p_{uv}$, and therefore the terms $\frac{1}{\rho_0}\frac{\partial\overline{p'u'}}{\partial z}$ and $\frac{1}{\rho_0}(\frac{\partial\overline{p'u'}}{\partial r}+\frac{\partial\overline{p'v'}}{\partial z})$ can be dropped from the equations in the self-similarity analysis (see also Ref. [25]). By exploring the symmetry groups, we identify functional forms of streamwise scaling laws of flow variables theoretically. Note that classical power-law scalings are results of stretching symmetry groups of flow variables. In particular, we identify whether there exist any other forms of similarity scaling laws or any other power-law scaling of turbulence quantities other than the classical power-law scaling. And if other forms exist, what are the symmetry groups underneath the non-power-law scaling? From the analysis, we found that for the turbulent axisymmetric plume at the infinite-Reynolds-number limit, the various flow variables evolve through the scaling symmetry transformations corresponding to the parameters $a_1, a_2 \in \mathbb{R}$, and translation symmetry transformation with parameter $a_0 \in \mathbb{R}$ satisfying the invariance of the boundary conditions Eq. (2), constancy of the buoyancy flux Eq. (7c), and the scaling relation $\overline{\theta'^2} \sim \theta^2$. See the Appendix for the infinitesimal and global forms of the transformations of the variables. Equations (1a), (1b), (1c), (3), and (5) are form invariant under the transformations Eqs. (A2a), (A2b), and (A2c). The analysis reveals that the two stretching parameters are connected with the evolvement of turbulent flow quantities and the translation parameter along with one of the stretching group parameter decide the virtual origin of plume. For self-preservation $\overline{u}$ and θ must maintain the invariance of boundary conditions Eq. (2) at $r = 0$, that is, the centerline velocity $\overline{u}(z, 0)$ denoted by $\overline{u}_c$ and centerline temperature difference $\theta(z, 0)$ denoted by θ_c must satisfy the following equations:

$$\xi_z \frac{d\overline{u}_c}{dz} - \eta_{\overline{u}} = 0, \tag{8}$$

$$\xi_z \frac{d\theta_c}{dz} - \eta_\theta = 0, \tag{9}$$

where $\xi_z = a_0 + a_1 z$, $\eta_{\overline{u}} = (a_1 - 2a_2)\overline{u}/3$, and $\eta_\theta = -(a_1 + 4a_2)\theta/3$ are the infinitesimal transformations of z coordinate, $\overline{u}$, and θ, respectively. It is found that when a_0, a_1, and a_2 are nonzero then the above equations will hold if both $\overline{u}_c$ and θ_c obey a power-law variation with the vertical height, while when $a_1 = 0$ then they must obey an exponential law.

The present analysis mainly focused on the axial scaling of the flow variables. Note that $\overline{w'^2}$, $\overline{v'w'^2}$, $\overline{u'w'^2}$, and ϵ_w, respectively, admit the same symmetry transformations as $\overline{v'^2}$, $\overline{v'^3}$, $\overline{u'v'^2}$, and ϵ_v (see the Appendix). Hence, they will scale in the same way with the vertical(axial) distance and are equal on the centerline in the present analysis for the axisymmetric flow. So, we do not discuss the scaling laws of the variables $\overline{w'^2}$, $\overline{v'w'^2}$, $\overline{u'w'^2}$, and ϵ_w in the rest of the analysis.

B. Self-preserving solutions

We obtain self-preserving solutions of the form $\mathbf{U} = \mathbf{U_s}(z) f_i(\tau)$ at the infinite-Reynolds number limit, where $\mathbf{U} \equiv (\overline{u}, \overline{v}, \theta, \overline{u'v'}, \overline{v'\theta'}, \overline{u'\theta'}, \overline{u'^2}, \overline{v'^2}, \overline{w'^2}, \overline{k_\theta}, (\overline{u'^2} - \overline{v'^2}), \epsilon_u, \epsilon_v, \epsilon_w, \epsilon_\theta, p_u, p_v, p_w, p_{uv}, \epsilon_{uv}, \overline{u'^2v'}, \overline{v'w'^2}, \overline{u'v'^2}, \overline{v'^3}, \overline{k}, \overline{v'k + p'v'/\rho_0}, \epsilon)$. Here $\mathbf{U_s}$ are scales which are functions of z independent of r and φ and f_i, $i = 1, 2, \ldots, 27$ are self-preserving functions of the similarity variable $\tau = r/\delta(z)$, where $\delta(z)$ is a function of z independent of r and φ. Thus, the solutions are of the forms

$$\overline{u} = \overline{u}_s f_1(\tau), \overline{v} = \overline{v}_s f_2(\tau), \theta = \theta_s f_3(\tau), \overline{u'v'} = (\overline{u'v'})_s f_4(\tau), \overline{v'\theta'} = (\overline{v'\theta'})_s f_5(\tau),$$
$$\overline{u'\theta'} = (\overline{u'\theta'})_s f_6(\tau), \ldots, (\overline{u'^2} - \overline{v'^2}) = (\overline{u'^2} - \overline{v'^2})_s f_{11}(\tau), \ldots \text{ and so on.} \tag{10}$$

It is important to note here that the functional forms of $\mathbf{U_s}$ and $\delta(z)$ depend on the values of symmetry group parameters a_0, a_1, and a_2 maintaining the constancy of buoyancy flux B_F. In the case when $a_0 \neq 0, a_1 \neq 0$, and $a_2 \neq 0$, we obtain the general power-law self-preserving solutions $\mathbf{U} = \mathbf{U_s} f_i(\tau)$, where the scaling function $\mathbf{U_s}$ is of power-law form with the exponent depending on the ratio a_2/a_1 and the similarity variable $\tau = r/\delta(z)$, where $\delta(z) = z_0[(z + a)/z_0]^{a_2/a_1}$ with $a = a_0/a_1$ and z_0 is some initial width of the flow. The streamwise scaling law of axial and radial velocities $\overline{u}$ and $\overline{v}$, mean temperature difference θ, turbulent shear stress $\overline{u'v'}$, and the turbulent axial and radial heat fluxes $\overline{u'\theta'}$, $\overline{v'\theta'}$ are obtained as

$$\overline{u}_s = \gamma \left(\frac{B_F}{z_0}\right)^{1/3} \left[\frac{z+a}{z_0}\right]^{\left(\frac{1}{3} - \frac{2a_2}{3a_1}\right)}, \quad \overline{v}_s = \gamma \left(\frac{B_F}{z_0}\right)^{1/3} \left[\frac{z+a}{z_0}\right]^{\left(\frac{-2}{3} + \frac{a_2}{3a_1}\right)},$$
$$\theta_s = \frac{\gamma^2}{(g\beta) z_0} \left(\frac{B_F}{z_0}\right)^{2/3} \left[\frac{z+a}{z_0}\right]^{-\left(\frac{1}{3} + \frac{4a_2}{3a_1}\right)}, \quad (\overline{u'v'})_s = \gamma^2 \left(\frac{B_F}{z_0}\right)^{2/3} \left[\frac{z+a}{z_0}\right]^{-\left(\frac{1}{3} + \frac{a_2}{3a_1}\right)},$$
$$(\overline{u'\theta'})_s = \frac{\gamma^3}{(g\beta) z_0} \left(\frac{B_F}{z_0}\right) \left[\frac{z+a}{z_0}\right]^{-\frac{2a_2}{a_1}}, \quad (\overline{v'\theta'})_s = \frac{\gamma^3}{(g\beta) z_0} \left(\frac{B_F}{z_0}\right) \left[\frac{z+a}{z_0}\right]^{-\left(1 + \frac{a_2}{a_1}\right)}, \tag{11}$$

where γ is dimensionless parameter that may depend on source conditions and u_0 is a constant velocity scale at z_0. From above we can see that the stretching group parameters a_1 and a_2 by their ratio a_2/a_1 mainly decide how the flow is evolving, while the translation parameter a_0 along with parameter a_1 decide the virtual origin by their ratio $a = a_0/a_1$. Note that the present theoretical study shows that the ratio a identifying the virtual origin must be same for all flow quantities for the self-similarity of the equations. However, in literature, the experimental studies reported different values of virtual origins for different flow quantities. The measurement of Cafiero and Vassilicos [22] is an exception. The kinematic volume and kinematic momentum fluxes from their definitions and using the above scaling laws are obtained as

$$Q(z) = \gamma z_0^2 \left(\frac{B_F}{z_0}\right)^{1/3} \left[\frac{z+a}{z_0}\right]^{\frac{1}{3}\left(1 + \frac{4a_2}{a_1}\right)} I_1, \tag{12}$$
$$M(z) = \gamma^2 z_0^2 \left(\frac{B_F}{z_0}\right)^{2/3} \left[\frac{z+a}{z_0}\right]^{\frac{2}{3}\left(1 + \frac{a_2}{a_1}\right)} (I_2 + I_f), \tag{13}$$

where $I_1 = 2\pi \int_0^\infty f_1 \tau d\tau$, $I_2 = 2\pi \int_0^\infty f_1^2 \tau d\tau$, and $I_f = 2\pi \int_0^\infty f_{11} \tau d\tau$. The turbulent normal stresses and intensity of thermal fluctuation scale with the vertical distance as

$$(\overline{u'^2})_s = \left(\frac{\gamma^3 B_F}{z_0}\right)^{2/3} \left[\frac{z+a}{z_0}\right]^{\frac{2}{3} - \frac{4a_2}{3a_1}}, \quad (\overline{v'^2})_s = \left(\frac{\gamma^3 B_F}{z_0}\right)^{2/3} \left[\frac{z+a}{z_0}\right]^{\left(-\frac{4}{3} + \frac{2a_2}{3a_1}\right)} = (\overline{w'^2})_s,$$
$$(\overline{k_\theta})_s = \frac{\left(\frac{\gamma^3 B_F}{z_0}\right)^{4/3}}{(g\beta z_0)^2} \left[\frac{z+a}{z_0}\right]^{-2\left(\frac{1}{3} + \frac{4a_2}{3a_1}\right)}. \tag{14}$$

The turbulent kinetic energy $\overline{k}_s = (\overline{u'^2})_s = \overline{u}_s^2$. Note that the Reynolds stress tensor components do not scale as same power law of vertical distance unless $a_1 = a_2$. The components of homogeneous dissipation and the dissipation of thermal fluctuation scale with z as

$$(\epsilon_u)_s = \frac{\gamma^3}{z_0}\frac{B_F}{z_0}\left[\frac{z+a}{z_0}\right]^{-\frac{2a_2}{a_1}}, \quad (\epsilon_v)_s = \frac{\gamma^3}{z_0}\frac{B_F}{z_0}\left[\frac{z+a}{z_0}\right]^{-2} = (\epsilon_w)_s, \tag{15}$$

$$(\epsilon_\theta)_s = \frac{\gamma^5}{(g\beta)^2 z_0^3}\left(\frac{B_F}{z_0}\right)^{5/3}\left[\frac{z+a}{z_0}\right]^{-\left(\frac{4}{3}+\frac{10a_2}{3a_1}\right)}. \tag{16}$$

The streamwise scaling of turbulent energy dissipation $\epsilon_s \sim (\epsilon_u)_s$. Thus, for constant ambient temperature T_a, the scaling laws of dissipation components ϵ_v and ϵ_w with the vertical distance z are same and fixed, while that of ϵ_u and ϵ_θ vary with varying values of the ratio a_2/a_1. Moreover, in general, the streamwise scaling laws of the components of dissipation are not same. They are same only when the ratio $a_2/a_1 = 1$ and additional information are required to determine the condition under which $a_2/a_1 = 1$ holds. We found that in general, $(\epsilon_u)_s/(\epsilon_v)_s = [(z+a)/z_0]^{2(1-a_2/a_1)}$. The pressure-strain components scale with z as $p_u = \frac{\gamma^3}{z_0}\frac{B_F}{z_0}[(z+a)/z_0]^{-\frac{2a_2}{a_1}} f_{16}(\tau)$, $p_v = \frac{\gamma^3}{z_0}\frac{B_F}{z_0}[(z+a)/z_0]^{-2} f_{17}(\tau)$, and $p_w = \frac{\gamma^3}{z_0}\frac{B_F}{z_0}[(z+a)/z_0]^{-2} f_{18}(\tau)$. We will show later that the relation $p_u + p_v + p_w = 0$ is not free of the vertical distance and hence not completely self-similar when $a_2 \neq a_1$. What does it imply physically? It clearly indicates that the role of the components of pressure-strain-rate tensor is important and have significant effects (see also Ref. [34]). Further, the nonsimilarity implies nonequilibrium of flow components and non-Kolmogorov turbulence. The above expressions for flow variables clearly indicate the role of two stretching group parameters in the evolution of turbulent flow. While evolving the scaling of flow variables are connected with each other. We will now discuss this in the following section.

C. Scaling relations

Scaling relations among the flow quantities are significant as it may assist in the modeling of flow variables to close the underdetermined equations. But before delving into the scaling relationships, we obtain the centerline scaling laws at $\tau = 0$ (that is at $r = 0$) of mean axial velocity and mean temperature difference and the spreading rates. The centerline velocity $\overline{u}_c$ and centerline temperature difference θ_c are obtained as

$$\overline{u}_c = K_u\left(\frac{B_F}{z_0}\right)^{1/3}\left[\frac{z+a}{z_0}\right]^{\frac{1}{3}\left(1-\frac{2a_2}{a_1}\right)}, \tag{17}$$

$$\theta_c = \frac{K_\theta}{(g\beta)z_0}\left(\frac{B_F}{z_0}\right)^{2/3}\left[\frac{z+a}{z_0}\right]^{-\frac{1}{3}\left(1+\frac{4a_2}{a_1}\right)}, \tag{18}$$

where $K_u = \gamma f_1(0)$ and $K_\theta = \gamma^2 f_3(0)$. $\overline{u}_c$ and θ_c agree with conventional results when $a_2/a_1 = 1$ (see Sec. IV B 1). The plume velocity $1/n$-width $\delta_{u/n}$ is defined by $\overline{u}(z, \pm\delta_{u/n}) = \overline{u}_c/n = \overline{u}_s f_1(0)/n$ and the plume temperature $1/n$-width $\delta_{\theta/n}$ is defined by $\theta(z, \pm\delta_{\theta/n}) = \theta_c/n = \theta_s f_3(0)/n$ and are obtained as

$$\frac{\delta_{u/n}}{z_0} = b_{u/n}\left[\frac{z+a}{z_0}\right]^{\frac{a_2}{a_1}}, \tag{19}$$

$$\frac{\delta_{\theta/n}}{z_0} = b_{\theta/n}\left[\frac{z+a}{z_0}\right]^{\frac{a_2}{a_1}}. \tag{20}$$

Both the $1/n$-widths evolve as a_2/a_1 power of vertical distance above the virtual origin. However, they differ for different values of the coefficients $b_{u/n}$ and $b_{\theta/n}$. In jets and plumes, the local widths usually grow with distance from source. This is possible here only if the ratio $a_2/a_1 > 0$. Moreover, $a_2/a_1 < 0$ would imply decay of local width with vertical distance that is not physically plausible. So here we consider $a_2/a_1 > 0$.

The plume velocity and temperature $1/n$-widths spreading rates are obtained as

$$\frac{d\delta_{u/n}}{dz} = b_{u/n}\frac{a_2}{a_1}\left[\frac{z+a}{z_0}\right]^{(-1+\frac{a_2}{a_1})}, \quad \frac{d\delta_{\theta/n}}{dz} = b_{\theta/n}\frac{a_2}{a_1}\left[\frac{z+a}{z_0}\right]^{(-1+\frac{a_2}{a_1})}. \tag{21}$$

Thus, spreading rates of velocity and temperature difference $1/n$-widths are decreasing for $0 < a_2/a_1 < 1$, are constants for $a_2/a_1 = 1$, and are increasing for $a_2/a_1 > 1$. For $a_2/a_1 = 1$, the velocity and temperature difference $1/n$-widths grow linearly but they differ for different rate of spreadings $b_{u/n}$ and $b_{\theta/n}$. It should be noted that the experimental measurements of planar jet in Ref. [22] showed jet width is always growing although its rate of spreading may decrease with increasing streamwise distance. This is also established theoretically in [21]. On the contrary, Refs. [23,24] suggested a possible growth in spreading rate of planar jet with increasing distance from source.

The local Reynolds number Re_δ is expressed by

$$\mathrm{Re}_\delta = \frac{\overline{u}_s\delta}{\nu} \propto \gamma z_0 u_0\left[\frac{(z+a)}{z_0}\right]^{\frac{1}{3}+\frac{a_2}{3a_1}}. \tag{22}$$

We see that Re_δ is increasing with increasing vertical distance for $a_2/a_1 > -1$. While plume velocity and temperature difference widths would be increasing with streamwise distance only if $a_2/a_1 > 0$. Nevertheless, we consider the ratio $a_2/a_1 > 0$ so that both the plume widths and Re_δ increase with increasing vertical distance.

From the above form of the solutions, we can relate the streamwise (s) scaling of flow variables as

$$\begin{aligned} &\overline{v}_s \sim \overline{u}_s\frac{d\delta}{dz}, \quad g\beta\theta_s \sim \frac{\overline{u}_s^2}{\delta}\frac{d\delta}{dz}, \quad (\overline{u'^2} - \overline{v'^2})_s \sim \overline{u}_s^2,\\ &\overline{u'v'}_s \sim \overline{u}_s^2\frac{d\delta}{dz}, \quad (\overline{v'\theta'})_s \sim \overline{u}_s\theta_s\frac{d\delta}{dz}, \quad (\overline{u'\theta'})_s \sim \overline{u}_s\theta_s,\\ &(\overline{u'^2})_s \sim \overline{u}_s^2, \quad (\overline{v'^2})_s \sim \overline{v}_s^2 \sim (\overline{w'^2})_s, \quad (\overline{k_\theta})_s \sim \theta_s^2. \end{aligned} \tag{23}$$

It is to be noted that the modeling of the plume statistical quantities for the closure should be done keeping in mind that the boundary conditions and the above streamwise scaling relations hold.

1. Turbulence dissipation scaling

As discussed in Sec. I, the dissipation laws are decisive in identifying the scaling laws of turbulent flows. Using the scaling relationships Eq. (23) and the axial scaling laws obtained in the previous section, we found scaling relationships among the dissipation components, Reynolds stresses, and plume velocity and temperature $(1/n)$ widths as follows:

$$(\epsilon_u)_s = C_{\epsilon_u}\frac{(\overline{u'^2})_s^{3/2}}{\delta_{u/n}}, \quad (\epsilon_v)_s = \frac{(\overline{v'^2})_s^{3/2}}{\delta_{u/n}}, \quad \text{and } (\epsilon_w)_s = (\epsilon_v)_s, \tag{24a}$$

$$(\epsilon_\theta)_s = C_{\epsilon_\theta}\frac{\overline{k_\theta}(\overline{u'^2})_s^{1/2}}{\delta_{\theta/n}}. \tag{24b}$$

The dissipation coefficient C_{ϵ_u} ($C_{\epsilon_u} \propto C_{\epsilon_\theta}$) varies with local velocity spreading rate $d\delta_{u/n}/dz$ given by

$$C_{\epsilon_u} \propto \frac{d\delta_{u/n}}{dz}. \tag{25}$$

Note that the dissipation coefficient C_ϵ of turbulent energy dissipation ϵ is proportional to C_{ϵ_u} as $\epsilon_s \propto (\epsilon_u)_s$. Now since the local Reynolds number Re_δ is increasing with increasing vertical distance z for $a_2/a_1 > 0$, we can express the dissipation coefficient C_{ϵ_u} as

$$C_{\epsilon_u} \propto \left(\frac{\mathrm{Re}_G}{\mathrm{Re}_\delta}\right)^m, \quad \text{with } m = \frac{3(a_1 - a_2)}{(a_1 + a_2)}, \quad \text{where } a_2 \neq -a_1. \tag{26}$$

Thus, $\frac{d\delta_{u/n}}{dz} \propto (\frac{\mathrm{Re}_G}{\mathrm{Re}_\delta})^m$. Here the global (inlet) Reynolds number $\mathrm{Re}_G = u_0 z_0/\nu$. The normal stresses $(\overline{u'^2})_s$ and $(\overline{v'^2})_s$ are related by

$$(\overline{v'^2})_s \propto (C_{\epsilon_u})^2 (\overline{u'^2})_s. \tag{27}$$

Thus, we can see that the ratio $a_2/a_1 = 1$ only if $m = 0$. Both the dissipation coefficients C_{ϵ_u} and C_{ϵ_θ} are constants and from Eq. (24a), $(\epsilon_u)_s \sim (\epsilon_v)_s \sim (\epsilon_w)_s$ in agreement with the Kolmogorov equilibrium dissipation law for $m = 0$. The components of normal stress tensor scale in the same way, that is, $(\overline{u'^2})_s \sim (\overline{v'^2})_s \sim (\overline{w'^2})_s$. Again for $m \neq 0$ and $a_2/a_1 \neq 1$, both the dissipation coefficients vary with local Reynolds number raised to a power $-m$ and as power m of the global Reynolds number, and so incomplete similarity holds. The above analysis reveals that the ratio a_2/a_1 of two stretching group parameters is directly involved in the evolvement of turbulent flow and also establishes a relation between self-similarity and Kolmogorov equilibrium law when $a_2/a_1 = 1$, while the ratio $a_2/a_1 \neq 1$ gives a nonsimilarity in the flow resulting non-Kolmogorov, nonequilibrium law.

Note that if the stretching parameter $a_1 = 0$ but $a_0 \neq 0$ and $a_2 \neq 0$ then the flow variables $\mathbf{U_s}$ exhibit exponential scaling laws and self-preserving functions f_i are functions of $\tau = r/\delta(z)$ with $\delta(z) = z_0 \exp[a_2 z/a_0 z_0]$. Note that in this case all flow variables undergo a stretching transformation with parameter a_2; however, the coordinate z undergoes translation without any stretching. The equations in this case are form invariant under one translation (a_0) and one stretching (a_2) group of transformations. Although, the exponential streamwise scaling laws of flow variables $[\mathbf{U_s}(z)]$ satisfy the scaling relationships given in Eq. (23), the dissipation laws Eqs. (24a) and (24b) hold with the dissipation coefficients $C_{\epsilon_u} \sim C_{\epsilon_\theta} \propto (\frac{\mathrm{Re}_G}{\mathrm{Re}_\delta})^m$, where $m = -3$.

Until now, we have obtained general scaling laws of flow variables with the rise of vertical distance under constant buoyancy flux and zero buoyancy frequency. However, the dissipation laws of Reynolds stress tensor, which may be either Kolmogorov or non-Kolmogorov, will determine the exact scaling laws for the specific flow.

D. Pressure-strain-rate equation for non-Kolmogorov turbulence

In the previous section, we identified new scaling laws for $m \neq 0$, that is, for $a_2 \neq a_1$ and the conventional scalings were obtained when complete self-similarity holds for $m = 0$ implying $a_2 = a_1$. The main limitation of analyzing only the TKE equation is that one overlooks the scaling behavior of pressure-strain-rate terms (see Ref. [9]). This is because that the components of pressure-strain-rate tensor do not appear in the TKE equation. However, the complete similarity of a free shear flow can be maintained if also the equation which results due to the sum of pressure-strain-rate components p_u, p_v, and p_w remains self-similar. The equation for pressure-strain-rate components is

$$p_u + p_v + p_w = 0. \tag{28}$$

We already found the solutions of $p_u = (B_F \gamma^3/z_0^2)[(z+a)/z_0]^{-2a_2/a_1} f_{16}(\tau)$, $p_v = (B_F \gamma^3/z_0^2)[(z + a)/z_0]^{-2} f_{17}(\tau)$, and $p_w = \frac{\gamma^3}{z_0}\frac{B_F}{z_0}[(z+a)/z_0]^{-2} f_{18}(\tau)$. Therefore, from the above equation we write

$$f_{16} + j(z)(f_{17} + f_{18}) = 0, \quad \text{where } j(z) = \left[\frac{z+a}{z_0}\right]^{-2(1-\frac{a_2}{a_1})}. \tag{29}$$

We can see that Eq. (29) is not completely free of the streamwise distance z until $a_2/a_1 = 1$. Hence, it is nonsimilar when $a_2/a_1 \neq 1$, that is, $m \neq 0$ and we call this situation "non-Kolmogorov." Thus, non-Kolmogorov dissipation implies quasiequilibrium or pseudoequilibrium in free shear turbulent flows. The value of the ratio $a_2/a_1 \in (0, 1]$. For $0 \leqslant a_2/a_1 < 1$, the function $j(z)$ decays with vertical distance z and finally vanishes. In this case, Eq. (28) holds if the self-preserving function $f_{16} = 0$ when $j(z)$ is negligible. Again, if $j(z)^{-1}$ is negligible then the function $f_{17} = -f_{18}$. When $m = 0$ (that is, $a_2/a_1 = 1$), $j(z) = 1$ which implies an approximately equilibrium distribution of energy in various components and Eq. (28) becomes self-similar. We conclude that there exists a region where non-Kolmogorov theory holds and is due to nonsimilarity of the pressure-strain-rate equation and nonequilibrium in streamwise scaling of Reynolds stress tensor and dissipation tensor. Note that the importance of the pressure-strain-rate equation was also stressed by Johansson *et al.* [34] in determining the streamwise scaling laws.

IV. SELF-PRESERVING PROFILE FUNCTIONS

For the solutions of the form of Eq. (10) with the streamwise scaling laws Eq. (11) and assuming the profile function $f_1(\tau) = g'/\tau$, where $g' = dg(\tau)/d\tau$ is a function of τ, the self-similar forms of Eqs. (1a), (1b), and (1c) at the infinite-Reynolds-number limit can be obtained as

$$f_2(\tau) = \left(\frac{3q-1}{4}\right)g' - \frac{qg}{\tau}, \tag{30a}$$

$$\frac{1-q}{2}\frac{g'^2}{\tau} - qg\left(\frac{g'}{\tau}\right)' = \tau f_3 - (\tau f_4)' + \left\{(q-1)\tau f_{11} + \frac{(3q-1)}{4}\tau^2 f_{11}'\right\}, \tag{30b}$$

$$-q(gf_3)' = -(\tau f_5)' + \left\{\frac{3q-1}{2}\tau f_6 + \frac{3q-1}{4}\tau^2 f_6'\right\}, \tag{30c}$$

where $q = (\frac{1}{3} + \frac{4a_2}{3a_1})$. Here f_i' $(= df_i/d\tau)$, f_i'' $(= d^2 f_i/d\tau^2)$, and so on are order derivatives, $i = 1, 2, \ldots, 11$. The boundary conditions Eq. (2) written in self-similarity forms are

$$f_1' = 0,\ f_2 = 0,\ f_4 = 0,\ \text{and } f_5 = 0 \text{ at } \tau = 0 \text{ and } f_1 = 0 = f_3 \text{ as } \tau \to \infty. \tag{31}$$

Thus, for $f_1 = g'/\tau$ the boundary conditions $f_1' = 0$ and $f_2 = 0$ at $\tau = 0$ imply $g' = 0$ and $g = 0$. The above equations are not closed and so modellings are needed to determine the functions f_i, $i = 1, 2, \ldots, 11$.

A. Closure models maintaining symmetry

We must model the flow quantities which retain symmetry of the equation, so it is called symmetry-based modeling. The equations are unclosed and additional models are required to solve them. Note that the additional models can break the symmetries under which the unclosed equations are form invariant. The classical generalized eddy viscosity hypothesis for the Reynolds stresses is given by $\overline{u_i'u_j'} = (2/3)\overline{k}\delta_{ij} - \nu_t(\partial\overline{u_i}/\partial x_j + \partial\overline{u_j}/\partial x_i)$, which is valid for isotropic and weakly anisotropic free shear flows in which at least the streamwise scaling laws are isotropic. For non-Kolmogorov free shear flows maintaining incomplete similarity, the eddy viscosity hypothesis is not complete and not accurate. Note that classically isotropic eddy viscosity is specified by $\nu_t \sim \overline{u}l$, l is the characteristic length scale of the flow and therefore is valid only for equilibrium dissipations of Reynolds stresses with plume height. Layek and Sunita [19,21,25] gave a modified eddy viscosity $\nu_t \sim \overline{u}ldl/dx$, which worked well for the Reynolds shear stress $-\overline{u'v'}$ when either the Kolmogorov equilibrium dissipation or the non-Kolmogorov dissipation holds. However, since $\overline{u'^2}$ and $\overline{v'^2}$ scale differently, and the term $(\overline{u'^2} - \overline{v'^2})_s \sim (\overline{u'^2})_s$, the isotropic eddy viscosity hypothesis according to which $(\overline{u'^2} - \overline{v'^2}) = -4\nu_t\partial\overline{u}/\partial z - 2\nu_t\overline{v}/r$ is not valid for both the classical and the modified forms of ν_t when non-Kolmogorov dissipation holds. Cafiero *et al.* [35] found that when $m = 1$ the mixing length $l_m \sim (\mathrm{Re}_G/\mathrm{Re}_\delta)^{1/2}\delta$, while the eddy viscosity hypothesis may hold provided eddy viscosity is unvarying in both the streamwise and cross-stream directions. The existing experimental measurements reported that the term involving $(\overline{u'^2} - \overline{v'^2})$ is very small in the mean momentum equation, so the terms within the braces in Eq. (30b) can be neglected. However, they found the gradient of radial turbulent heat flux in mean temperature difference equation not negligible and some measurements suggest that the term involving $(\overline{u'^2} - \overline{v'^2})$ is not negligible in kinetic energy productions. Note that the modified form of the eddy viscosity can hold under non-Kolmogorov dissipations when both the streamwise gradients of $(\overline{u'^2} - \overline{v'^2})$ and $\overline{u'\theta'}$ are negligible. It appears that the isotropic eddy viscosity hypothesis is not applicable to free shear flows when the non-Kolmogorov dissipation holds and the terms involving $(\overline{u'^2} - \overline{v'^2})$ are not negligible relative to the other terms in the mean equations and turbulent kinetic energy equations. The Reynolds stress equations can serve better in this case, nevertheless, they are also not closed and require modeling of turbulent diffusions, pressure-rate of strain tensor, etc., to determine the radial variations of the flow variables, that is, the functions $f_i(\tau)$ and are computationally difficult and costly. However, it is desirable to see how the profiles of mean flow quantities would behave when non-Kolmogorov scaling laws hold and how they differ from the profiles that correspond to Kolmogorov scaling. For that here we solve the mean continuity, momentum, and temperature equations with a closure model of Reynolds shear stress. There exist many crude models, viz. mixing length model, eddy viscosity model, etc., of the Reynolds shear stress in literature. Here we will analyze the equations under the modified eddy viscosity approach by neglecting the streamwise gradients of $(\overline{u'^2} - \overline{v'^2})$ and $\overline{u'\theta'}$.

B. Solutions for modified eddy viscosity hypothesis

The mean continuity, momentum, and temperature difference equations are solved by adopting the eddy viscosity hypothesis with the modified form of eddy viscosity $\nu_t \propto \overline{u}_c \delta d\delta/dz$ uniform in radial direction and by neglecting the terms within the braces in Eqs. (30b) and (30c). According to the eddy viscosity hypothesis $\overline{u'v'} = -\nu_t \partial\overline{u}/\partial r$ and $\overline{v'\theta'} = -\kappa_t \partial\theta/\partial r$, where $\kappa_t = \nu_t/\sigma_t$ and $\sigma_t = \mathrm{Pr}_t = (\overline{u'v'}\partial\theta/\partial r)/(\overline{v'\theta'}\partial\overline{u}/\partial r)$, is the constant turbulent Prandtl number when $\nu_t = \gamma B_F^{1/3}[(z+a)/z_0]^{-2/3+4a_2/3a_1}$ according to the modified form. Thus, we have $f_4 = -f_1' = -(g'/\tau)'$ and $f_5 = -f_3'/\sigma_t$, $f_3' = df_3/d\tau$. Now following Yih [7] from Eq. (30c) with terms within braces neglected and using $f_1 = g'/\tau$, where we choose the form of $g = A\omega\tau^2/(1+\omega\tau^2)$ and $f_5 = -f_3'/\sigma_t$, we obtain the forms of the solutions for the axisymmetric plume as

$$f_1 = \frac{2A\omega}{(1+\omega\tau^2)^2} \quad \text{and} \quad f_3 = \frac{B}{(1+\omega\tau^2)^{Aq\sigma_t/2}}. \tag{32}$$

The above forms of solutions hold for two possible choices of $Aq\sigma_t/2$. One for $Aq\sigma_t/2 = 4$, that is, $A = 8/q\sigma_t$, which implies $\sigma_t = 2$ independent of q from Eq. (30b) with $f_4 = -(g'/\tau)'$ and Eq. (6b) and the other for $Aq\sigma_t/2 = 3$, which implies

$$A = \frac{6}{q\sigma_t} \quad \text{and} \quad B = \frac{96\omega^2(3-2\sigma_t)}{q\sigma_t^2} \quad \text{with } \sigma_t = \frac{5q-1}{4q}. \tag{33}$$

We see that here σ_t depends only on q and hence its value is fixed for a given value of a_2/a_1. Since the buoyancy flux $B_F = B_{F_m}$ is a constant, therefore, for $\overline{u}$ and θ in Eq. (10) with $\overline{u}_s$ and θ_s given in Eq. (11), we obtain $\gamma^3 \int_0^\infty f_1 f_3 \tau d\tau = 1$ from the definition of buoyancy flux in Eq. (7c) and ignoring the second integral B_{F_f}. Using this relation for the above solutions of f_1 and f_3 with A, B and σ_t in Eq. (33), we obtain

$$\omega^2 = \frac{(-1+5q)^3}{9216\pi(1+q)\gamma^3} > 0 \text{ provided } q > 1/5, \text{ that is } a_2/a_1 > -1/10 \text{ and } \gamma > 0. \tag{34}$$

The existing experimental measurements reported the value of turbulent Prandtl number $\sigma_t \approx 1$, for example, in George and Shabbir [2] its value ranges from 0.7–1.0. Again, the theoretical study by Yih [7] found $\sigma_t = 1.1$. Therefore, here we may consider the solutions for $Aq\sigma_t/2 = 3$ with $1/2 < \sigma_t = (5q-1)/4q \lessapprox 1.1$, which also implies $0 < a_2/a_1 \leqslant 1$. Thus, from the above analysis, we found that the solutions of the axisymmetric plume in the unstratified ambient depend on two unknown parameters. One is the ratio of symmetry group parameters a_1 and a_2, and the other is the dimensionless parameter γ. The value of a_2/a_1 can be determined from the dissipation laws Eqs. (24a) and (24b) with dissipation coefficient Eq. (26) for different values of the exponent m. The parameter γ may depend on conditions at the source of the plume and can be determined from available experimental measurements. Now we discuss the scaling laws and the profile parameters under the dissipation relations with $m = 3(a_1 - a_2)/(a_1 + a_2)$ taking the specific values as follows.

1. Case 1: Kolmogorov dissipation region

As discussed in the previous section, the dissipation laws Eqs. (24a) and (24b) imply Kolmogorov equilibrium dissipation when the value of $m = 0$ and hence $a_2/a_1 = 1$. Consequently, $(\epsilon_u)_s = (\epsilon_v)_s = (\epsilon_w)_s \propto \frac{\gamma^3}{z_0}\frac{B_F}{z_0}[\frac{z+a}{z_0}]^{-2}$ and $(\epsilon_\theta)_s \propto (g\beta)^{-2}\frac{\gamma^5}{z_0^3}(\frac{B_F}{z_0})^{5/3}[\frac{z+a}{z_0}]^{-14/3}$. The Reynolds stress components scale in the same way with the vertical distance z, that is, $(\overline{u'^2})_s = (\overline{v'^2})_s = (\overline{w'^2})_s \sim (\overline{u})_s^2 \propto \gamma^2(\frac{B_F}{z_0})^{2/3}[\frac{z+a}{z_0}]^{-2/3}$ and $(\overline{u'v'})_s \sim (\overline{u})_s^2 d\delta_u/dz \propto \gamma^2(\frac{B_F}{z_0})^{2/3}[\frac{z+a}{z_0}]^{-2/3}$. In this case, the velocity and temperature $1/n$-widths, centerline mean axial velocity, and centerline mean temperature difference scale with the vertical distance z as

$$\frac{\delta_{u/n}}{z_0} = b_{u/n}\frac{z+a}{z_0}, \quad \frac{\delta_{\theta/n}}{z_0} = b_{\theta/n}\frac{z+a}{z_0}, \quad \overline{u}_c = K_u\left(\frac{B_F}{z_0}\right)^{1/3}\left[\frac{z+a}{z_0}\right]^{-\frac{1}{3}},$$
$$\theta_c = K_\theta\frac{(g\beta)^{-1}}{z_0}\left(\frac{B_F}{z_0}\right)^{2/3}\left[\frac{z+a}{z_0}\right]^{-\frac{5}{3}}. \tag{35}$$

The spreading rates $d\delta_{u/n}/dz = b_{u/n}$ and $d\delta_{\theta/n}/dz = b_{\theta/n}$ do not vary with axial (vertical) distance in agreement to the classical studies. However, there is no general agreement on whether the axial velocity width is wider than the temperature difference width or otherwise. Note that some experimental measurements (see Rouse *et al.* [6] and Papanicolaou and List [12]) calculated the value of $b_{\theta/2}$ (or $b_{\theta/e}$) higher than $b_{u/2}$ (or $b_{u/e}$), while others (George *et al.* [11], Shabbir and George [2]) found their behavior just the opposite and this is still controversial. Since $a_2/a_1 = 1$, the value of $q = 1/3 + 4a_2/3a_1 = 5/3$ and the solutions Eq. (32) hold for $\sigma_t = 11/10$, with

$$A = \frac{36}{11} \quad \text{and} \quad B = \frac{4608\omega^2}{121}, \quad \text{where } \omega^2 = \frac{1331}{9216\pi\gamma^3} > 0 \text{ for } \gamma > 0. \tag{36}$$

Comparisons with the experimental measurements Refs. [2,6,11,12,36,37] suggest the average value of $\gamma = 0.0165$ for which we obtain $b_{u/2} = 0.110832$, $b_{\theta/2} = 0.0877956$, $K_u = 2\gamma A\omega = 3.64183$, and $K_\theta = \gamma^2 B = 11.7893$ when $m = 0$. Thus, in the present study, we found that the velocity width is wider than the temperature difference width in agreement with the experimental measurements of Refs. [2,11,36] and are contrary to the measurements of Refs. [6,12,37] (see Table I).

The velocity and temperature difference ($1/e$) widths with spreading rate values of $b_{u/e} = 0.138702$ and $b_{\theta/e} = 0.108315$ are compared with measured data of Papanicolaou and List (PL) [12] in Fig. 2. The width z_0 is equivalent to diameter D in PL [12]. Also, comparisons of the evolutions of centerline mean axial velocity and centerline mean temperature difference given in Eq. (35) with the above values of K_u, K_θ, and virtual origin $a = -0.5z_0$ are shown in Figs. 2(c) and 2(d). We see that the results for temperature difference width, centerline mean axial velocity, and centerline mean temperature difference with same virtual origin ($a = [-0.5z_0, 2.5z_0]$) from the present theory agree well with the measured data, while the axial velocity width differs significantly for $z/z_0 > 40$. This is because in contradiction to the present study, $b_{u/e} < b_{\theta/e}$ in PL. Again, we can see from Table I that the centerline value of velocity is about 6.64% lower in SG94 [2] compared to present study but is larger in PL [12] by about 5.72% and in Ref. [36] by about 6.81% from the present study. However, the value is considerably higher in WL [37] by about 13.4% and in Ref. [6]

TABLE I. Comparison of mean flow parameters with the corresponding parameter for the curve fits of measured data in experiments

	$b_{u/2}$	$b_{\theta/2}$	K_u	K_θ
Rouse *et al.* [6]	0.084	0.095	4.7	11.0
Nakagome and Hirata [36]	0.12	0.105	3.89	11.5
Papanicolaou and List [12]	0.0877	0.093	3.85	14.28 or 11.1
Shabbir and George [2]	0.107	0.10	3.4	9.4
Wang and Law [37]	0.0874182	0.0907485	4.13	11.3
Present study $\gamma = 0.0165$				
$m = 0$ ($a_2/a_1 = 1, q = 5/3$)	0.110832	0.0877956	3.64183	11.7893
$m = 1/2$ ($a_2/a_1 = 5/7, q = 9/7$)	0.133626	0.105852	3.38443	8.72711
$m = 4/5$ ($a_2/a_1 = 11/19, q = 21/19$)	0.150026	0.118843	3.22012	7.27662
$m = 1$ ($a_2/a_1 = 1/2, q = 1$)	0.162503	0.128727	3.10576	6.4305

roughly by 29%. The centerline value K_θ of temperature difference in the present study is in good agreement to its value in Refs. [6,36,37] in comparison to SG94 [2] where it is substantially low by about 20.2%. The shape of the radial profiles calculated from the mean continuity, momentum, and temperature difference equations with the modified eddy viscosity closure are compared with measured data of Shabbir and George (SG94) [2] and Papanicolaou and List (PL) [12] in Fig. 3. We can see that the mean velocity profile of the present study agrees well about the centerline with SG94 [2] in comparison to PL [12]. The mean temperature difference profile although is in good agreement to Shabbir and George [2] and differs very small from PL [12]. Note that the difference of the calculated profile is very large from the fitted profile (not shown here) of Nakagome and Hirata [36]. The radial profile of radial velocity component is plotted and compared with measured data of Shabbir and George (SG94) [2] in Fig. 4. It is evident that the measured data and calculated profile has no agreement beyond $\tau = 0.10$. The same thing was also noted down by Shabbir and George [2] for the profile calculated by them from the equations. From Fig. 5, we see that the maximum of the nondimensionalized radial heat flux profile of the present study is 0.0317947 at $\tau = 0.0650883$, which is comparable to the maximum values 0.0290871 and 0.0312558, respectively, of the curve fits to the measured data of radial heat flux in Shabbir and George [2] and in Wang and Law [37], but is much higher than the peak value 0.020–0.025 reported by Papanicolaou and List [12]. However, note that about $\tau = 0.2$ the radial heat flux profile in the present theoretical study differs from Shabbir and George [2] and Wang and Law [37]. Again the profile for the turbulent shear stress has a maximum value 0.027236 at $\tau = 0.0770136$ which is comparable to the peak value 0.0262991 of the curve fit of the measured data in Shabbir and George [2] but is much higher than the peak value 0.0205363 of the curve fit to the measured data in Wang and Law [37]. The present nondimensionalized shear stress profile differs significantly from the measured data of

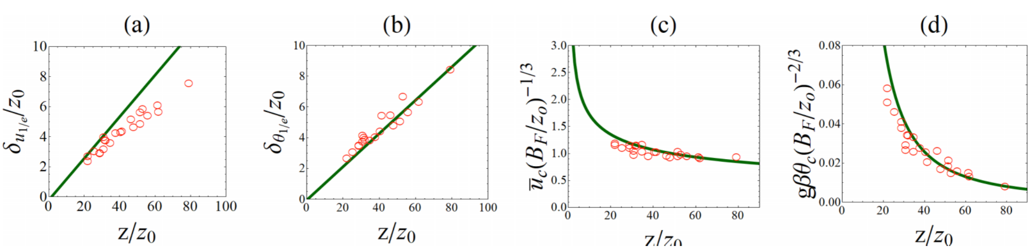

FIG. 2. Comparison of (a) velocity $1/e$ width and (b) temperature difference $1/e$ width and centerline evolution (c) mean axial velocity (d) mean temperature difference (solid curve) with $a = -0.5z_0$ when $m = 0$ with the measured data (○) of Papanicolaou and List (PL) [12].

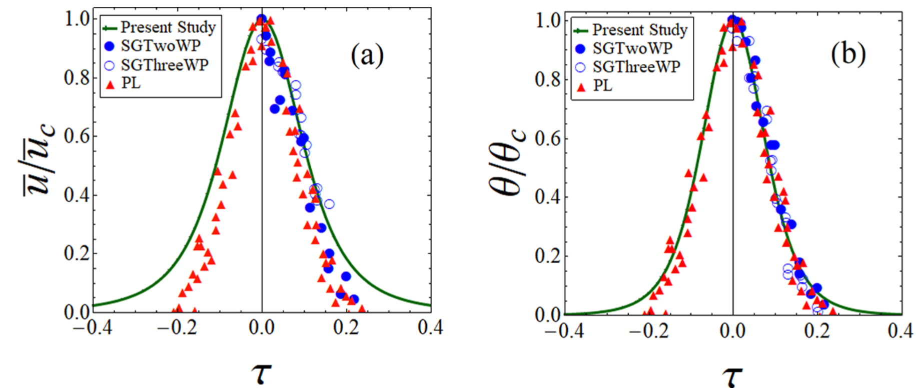

FIG. 3. Radial profiles of (a) mean axial velocity and (b) mean temperature difference normalized by their centerline value when $m = 0$ are compared with the measured data of normalized velocity and temperature/concentration profiles of Shabbir and George (SG94) [2] for both two and three wire probes and Papanicolaou and List (PL) [12]. The data of PL is obtained by digitization.

Shabbir and George [2] and Wang and Law [37] beyond $\tau = 0.15$. One of the reasons for the differences of solutions in the present study from experimental measurements is that we obtained the solutions by neglecting the term due to axial turbulent heat flux in the mean temperature difference equation. Note that here $\overline{u}_c^2 d\delta/dz$ is same as $\overline{u}_c^2$ and $\overline{u}_c\theta_c$ is same as $\overline{u}_c\theta_c d\delta/dz$ as $d\delta/dz = 1$ for $m = 0$ $(a_2/a_1 = 1)$. If the turbulent shear stress and radial heat flux are made dimensionless by $\overline{u}_c^2 d\delta_{u/2}/dz$ and $\overline{u}_c\theta_c d\delta_{\theta/2}/dz$, respectively, and plotted against τ, then the profiles peaks are higher multiplied by the factor $1/b_{u/2}$ and $1/b_{\theta/2}$, respectively, compared to when they were nondimensionalized by $\overline{u}_c^2 d\delta/dz$ and $\overline{u}_c\theta_c d\delta/dz$. We obtain $Q(z)B_F^{-1/3} z_0^{-2}(z+a)^{-5/3} = \gamma I_1 = 0.339292$, and $M(z)B_F^{-2/3} z_0^{-2}(z+a)^{-4/3} = \gamma^2 I_2 = 0.411881$, which is about 21% higher than the corresponding value 0.34 in Shabbir and George [2].

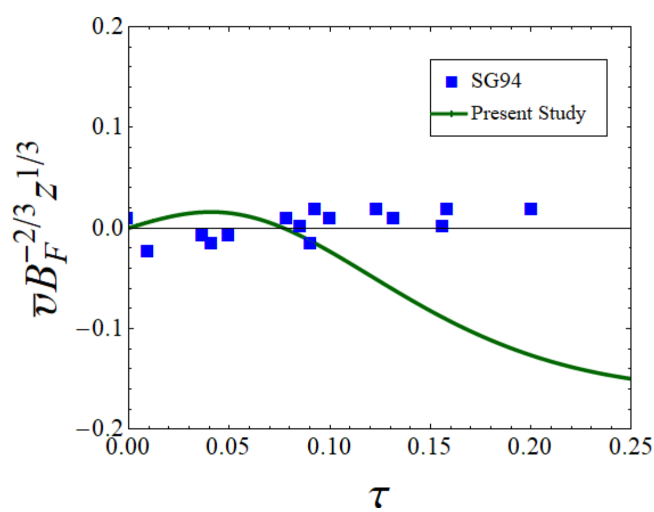

FIG. 4. Radial profile of mean radial velocity when $m = 0$ compared with the measured data of Shabbir and George (SG94) [2].

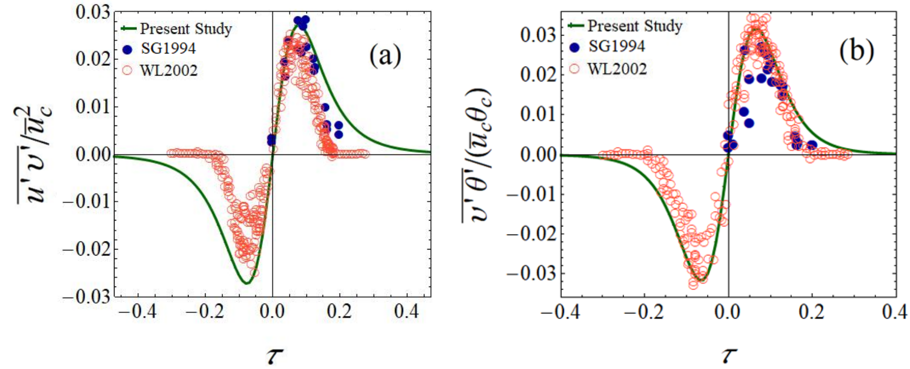

FIG. 5. Profiles of (a) shear stress made dimensionless by $\overline{u}_c^2$ and (b) radial heat flux made dimensionless by $\overline{u}_c\theta_c$ when $m = 0$ are compared with the measured data of Shabbir and George (SG94) [2] and Wang and Law (WL) [37]. The data of WL is obtained by digitization for comparison.

2. Case 2: Non-Kolmogorov dissipation $m \neq 0$

(i) Turbulent dissipation with $C_{\epsilon_u} \sim (\mathrm{Re}_G/\mathrm{Re}_\delta)$, that is, when $m = 1$ has been observed in many turbulent flows. Here when $m = 1$, then $a_1 = 2a_2$ and the dissipation laws Eqs. (24a) and (24b) are non-Kolmogorov (nonequilibrium), that is, $(\epsilon_u)_s \sim (\mathrm{Re}_G/\mathrm{Re}_\delta)(\overline{u'^2})_s^{3/2}/\delta_{u/n} \propto [\frac{z+a}{z_0}]^{-1}$, $(\epsilon_v)_s = (\epsilon_w)_s \sim (\overline{v'}^2)_s^{3/2}/\delta_{u/n} \propto \frac{\gamma^3}{z_0}\frac{B_F}{z_0}[\frac{z+a}{z_0}]^{-2}$, and $(\epsilon_\theta)_s \sim (\overline{k}_\theta)_s(\overline{u'^2})_s^{1/2}/\delta_{u/n} \propto (g\beta)^{-2}\frac{\gamma^5}{z_0^3}(\frac{B_F}{z_0})^{5/3}[\frac{z+a}{z_0}]^{-3}$. The Reynolds stress components are related by $(\overline{v'^2})_s = (\overline{w'^2})_s \sim (\mathrm{Re}_G/\mathrm{Re}_\delta)^2(\overline{u'^2})_s$ and $(\overline{u'v'})_s \sim (\mathrm{Re}_G/\mathrm{Re}_\delta)(\overline{u})_s^2$. In this case, the velocity and temperature $1/n$-widths, centerline mean streamwise velocity, and centerline mean temperature difference scale with the vertical distance z as

$$\frac{\delta_{u/n}}{z_0} = b_{u/n}\left[\frac{z+a}{z_0}\right]^{1/2}, \quad \frac{\delta_{\theta/n}}{z_0} = b_{\theta/n}\left[\frac{z+a}{z_0}\right]^{1/2}, \quad \overline{u}_c = K_u\left(\frac{B_F}{z_0}\right)^{1/3},$$
$$\theta_c = K_\theta\frac{(g\beta)^{-1}}{z_0}\left(\frac{B_F}{z_0}\right)^{2/3}\left[\frac{z+a}{z_0}\right]^{-1}. \tag{37}$$

Note that classical studies have found that the widths of planar jet, planar plume, and axisymmetric plume increase linearly with streamwise distance. However, from above results and from the studies of Cafiero and Vassilicos [22] and Refs. [19,21] we found that when $m = 1$ the $1/n$-widths in the planar jet, planar, and axisymmetric plumes increase as nonlinear power-law function of streamwise distance, however, they have different evolutions with power exponents as $2/3$, $2/5$, and $1/2$, respectively. As discussed in Sec. IV B 1, the present study gives value of $b_{u/n} > b_{\theta/n}$. However, in planar plume $b_{u/n} < b_{\theta/n}$. The spreading rates of velocity and temperature difference are given by

$$\frac{d\delta_{u/n}}{dz} = \frac{b_{u/n}}{2}\left[\frac{z+a}{z_0}\right]^{-1/2},$$
$$\frac{d\delta_{\theta/n}}{dz} = \frac{b_{\theta/n}}{2}\left[\frac{z+a}{z_0}\right]^{-1/2}. \tag{38}$$

We see that the spreading rates of both the velocity $1/n$-width and temperature difference $1/n$-width decrease as exponent $-1/2$ of the vertical distance in contrary to the classical studies of plume (see Fig. 6). However, this trend of spreading rates is in agreement to the recent experimental measurements of planar jet by Cafiero and Vassilicos [22], which reported an unconventional nonlinear decrease of jet spreading rate as $-1/3$ exponent of streamwise distance in the non-Kolmogorov dissipation region where turbulent energy dissipation coefficient $C_\epsilon \propto \mathrm{Re}_\delta^{-1}$. The spreading rate of

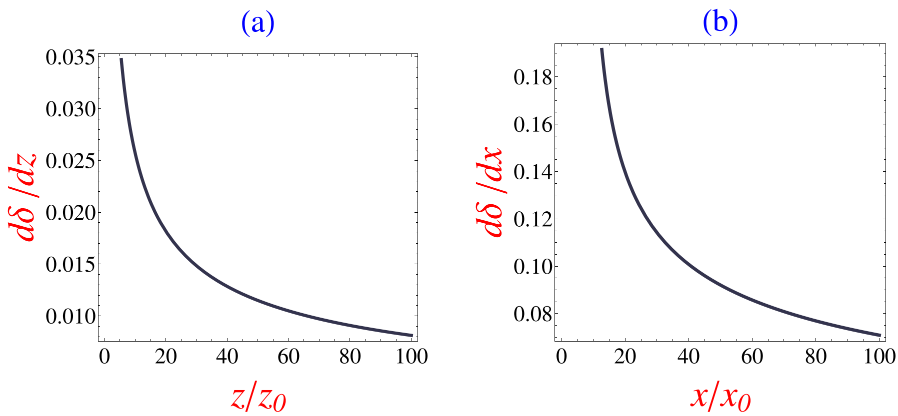

FIG. 6. Spreading rate of velocity half-width (a) axisymmetric plume, (b) planar jet in Refs. [21,22] when $m = 1$.

axisymmetric plume with respect to the power of the scaling function decays slowly compared to the spreading rate of planar plume where it decreases as $-3/5$ power of streamwise distance. This difference is mainly attributed to the configuration of the source of the flow. Since in this case $a_2/a_1 = 1/2$, the value of $q = 1/3(1 + 4a_2/a_1) = 1$ and the solutions Eq. (32) hold for $\sigma_t = 1$ with

$$A = 6 \text{ and } B = 96\omega^2, \quad \text{where } \omega^2 = \frac{1}{288\pi\gamma^3} > 0 \text{ for } \gamma > 0. \tag{39}$$

It should be noted that while experimental measurements of non-Kolmogorov turbulence dissipation have been performed in axisymmetric wake and planar jet, similar measurements have not yet been reported in plumes/buoyant jets. However, if we take the value of $\gamma = 0.0165$ also for $m = 1$ by considering that the source conditions are same for both $m = 0$ and 1, then we find the values $b_{u/2} = 0.162503$, $b_{\theta/2} = 0.128727$, $K_u = \gamma f_1(0) = 2\gamma A\omega = 3.10576$, and $K_\theta = \gamma^2 f_3(0) = \gamma^2 B = 6.4305$. We found that the value of $b_{u/2}$ in axisymmetric plume is greater than the planar plume, while the value of $b_{\theta/2}$ is smaller in axisymmetric plume compared to the planar plume value in Layek and Sunita [19]. So, velocity half-width grows faster, while temperature difference half-width after an initial faster growth evolves slowly in the axisymmetric plume compared to the planar plume in Layek and Sunita [19]. The centerline evolutions of mean axial velocity and mean temperature difference given in Eq. (37) with virtual origin set as $a = 0$ in this case are shown in Fig. 7. We see that the centerline mean axial velocity remains constant with increasing vertical distance z/z_0,

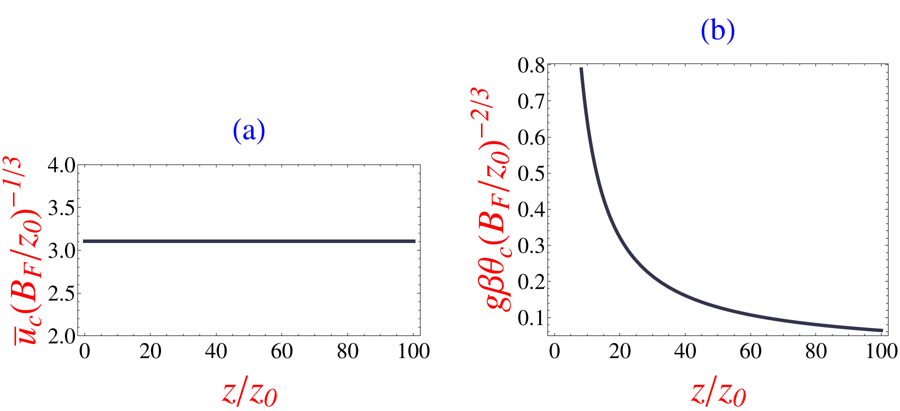

FIG. 7. Centerline evolution when $m = 1$ of (a) mean axial velocity (b) mean temperature difference.

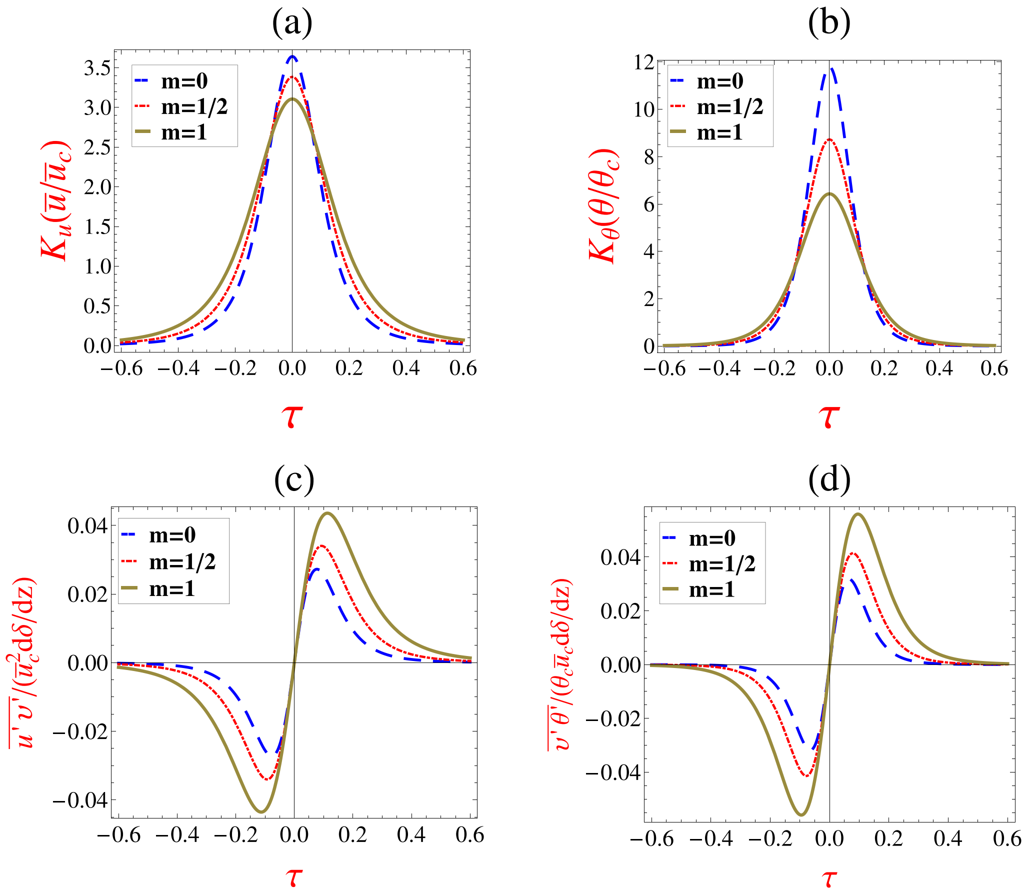

FIG. 8. Profiles of (a) mean axial velocity, (b)mean temperature difference, (c) Reynolds shear stress, and (d) radial heat flux when $m = 0$, $1/2$, and 1.

while centerline temperature difference decay as exponent -1 of z/z_0. The values of $b_{u/2}$ and $b_{\theta/2}$ are higher, the centerline value K_u is comparable, while the centerline value K_θ is much lower than the corresponding values for $m = 0$. Note that even if the source conditions are same for $m = 0$ and $m = 1$, the value of γ may be different for $m = 1$ depending on the distance of the region from the source where this scaling holds (see Ref. [21]). In that case, we may expect different values of $b_{u/2}$, $b_{\theta/2}$ and the centerline values of the radial profiles from the above. For the parameter values Eq. (39), the profile shapes are shown in Fig. 8. The value of $Q(z)B_F^{-1/3}z_0^{-5/3}[(z+a)/z_0]^{-1} = \gamma I_1 = 0.622035$ and $M(z)B_F^{-2/3}z_0^{-4/3}[(z+a)/z_0]^{-1} = \gamma^2 I_2 = 0.643964$.

(ii) When $m \in (0, 1)$ then $a_2/a_1 \in (1/2, 1)$, for which both the velocity and temperature difference width grow with increasing axial distance with power exponent lying in $(1/2, 1)$, while the rate of spreadings decrease with power exponent lying in $(-1/2, 0)$. The centerline axial velocity decay with power exponents lying in $(-1/3, 0)$, while centerline temperature difference decay with power exponents in the range $(-5/3, -1)$. The centerline values K_u and K_θ are maximum when $m = 0$ which decrease as m takes on values in (0,1) and are lowest for $m = 1$ (see Table I). The profiles for $m = 0$, $1/2$, and 1 are shown in Fig. 8. Although, the scale of $\delta(z) = z_0[(z+a)/z_0]^{a_2/a_1}$ changes with changing values of the ratio a_2/a_1 but with the transformation of the equations in similarity form with new similarity variable $\tau = r/\delta$, the changes will be discerned by the parameter $q = (1 + 4a_2/a_1)/3$ in Eqs. (30a), (30b), and (30c) and hence by a_2/a_1. In other words, the changes in scale in the original variables is absorbed by the parameter q in respect of the new similarity variables.

Note that non-Kolmogorov turbulent energy dissipation with dissipation coefficient $C_\epsilon \propto \mathrm{Re}_\delta^{-1/2}$ was reported in axisymmetric wake. In axisymmetric plume, $m = 1/2$ implies $a_2/a_1 = 5/7$. In this case, we have

$$\frac{\delta_{u/n}}{z_0} = b_{u/n}\left[\frac{z+a}{z_0}\right]^{5/7}, \quad \frac{\delta_{\theta/n}}{z_0} = b_{\theta/n}\left[\frac{z+a}{z_0}\right]^{5/7}, \quad \overline{u}_c = K_u\left(\frac{B_F}{z_0}\right)^{1/3}\left[\frac{z+a}{z_0}\right]^{-1/7},$$
$$\theta_c = K_\theta\frac{(g\beta)^{-1}}{z_0}\left(\frac{B_F}{z_0}\right)^{2/3}\left[\frac{z+a}{z_0}\right]^{-9/7}. \tag{40}$$

It is found that the radial profiles are narrowest for $m = 0$ and widest for $m = 1$. For a given value of γ, the peaks of turbulent shear stress and radial heat flux profiles are maximum when $m = 1$ which decrease as m takes on values less than 1 and are lowest when $m = 0$ for τ in the range [0,0.6]. Note that the maximum values of turbulent shear stress when $m = 1/2$ and 1, respectively, are 0.0340315 at $\tau = 0.0928522$ and 0.0435641 at $\tau = 0.112918$, while the maximum of turbulent radial heat flux when $m = 1/2$ and 1, respectively, are 0.0414003 at $\tau = 0.0784745$ and 0.0559412 at $\tau = 0.0954332$. For the maximum values when $m = 0$, see Sec. IV B 1.

Again, $a_2/a_1 \in (0, 1/2)$ correspond to values of $1 < m < 3$. In this case the plume widths are increasing, spreading rates and θ_c are decreasing, however, $\overline{u}_c$ is increasing as power law with the growth of axial distance which is in contrary to when $a_2/a_1 \in [1/2, 1]$, that is, $m \in [0, 1]$. The radial profiles for $m > 1$ are wider than those for $m = 1$, and the centerline values K_u and K_θ are smaller, but the peaks of turbulent shear stress and radial heat flux are larger compared to those for $m = 1$. Thus, we can say that the profiles are narrowest with maximum centerline values K_u and K_θ and lowest values of the peaks of shear stress and radial heat flux profiles when $m = 0$. The width of the profiles increases while the centerline values of axial velocity and temperature difference continually decrease and highest peaks of shear stress and radial heat flux profiles continually increase as we increase the value of m from 0. Note that available experimental measurements for the presence of nonequilibrium dissipation region in jet and wake flows reported $m \in [0, 1]$.

The analysis reveals that there is a difference in the radial profiles of flow quantities when $m \neq 0$ (non-Kolmogorov turbulence) from when $m = 0$ (Kolmogorov universal theory). However, nonequilibrium in vertical (axial) scaling laws and nonsimilarity of pressure-strain-rate equation are the main physical mechanism behind the non-Kolmogorov turbulence.

V. ENTRAINMENT COEFFICIENT AND ITS LINK WITH SPREADING RATES AND TURBULENT DISSIPATION

In the classical view entrainment is seen as an engulfment process. Along the interface between nonturbulent and the turbulent region there are growing vortex motion. These vortices give rise to engulfment of the ambient fluid leading to coherent structures of various types (see Ref. [38]). Entrainment typically occurs over a much larger time scales than turbulent timescales and its effects are obfuscated by turbulent fluctuations and transient effects. It requires the determination of a turbulent and nonturbulent regions which are arbitrary and hence subject to uncertainty. Nowadays there is growing an impetus to develop ideal microclimatic ventilation system which requires understanding entrainment characteristic of ventilation flow.

Morton *et al.* [16] following Taylor [15] proposed an entrainment approach to the problems of plume. They assumed that entrainment velocity v_e, that is, the radial velocity across $r = \delta(z)$, representing the boundary of the plume over which entrainment of ambient fluid into the plume occurs, is proportional to centerline mean streamwise velocity, that is, $\overline{v}_e = \alpha\overline{u}_c$, where α is the entrainment coefficient. For Kolmogorov dissipation, $\overline{v}_e$ and $\overline{u}_c$ scale in the same way and hence α is a constant (see also the Refs. [19,21]). However, in general, this is not true. Following Morton *et al.* [16] here we can write the conservation Eq. (6a) for nonconstant profiles (see Refs. [18,39])

as

$$\frac{dQ}{dz} = 2\alpha\sqrt{M}. \tag{41}$$

We found that in general $\alpha \sim d\delta(z)/dz$, and from the present study we know that $d\delta(z)/dz$ is not a constant but evolves as a function of vertical distance when dissipation laws hold with nonconstant C_{ϵ_u}, that is, when $m \neq 0$ and $a_2 \neq a_1$. For the classical scaling laws, using Priestley and Ball [40] conservation equation for mean energy, it was shown by Kaminskii *et al.* [14] in axisymmetric plume and Paillat and Kaminskii [17] in planar plume that α although is a constant in z but varies with the local Richardson number. Following them here we show that α can be related to the local Richardson number $\mathrm{Ri} = \frac{B_F Q^2}{M^{5/2}}$, which is a constant for $m = 0$ but evolves as a function of z when $m \neq 0$.

The integral form of mean kinetic energy equation is given by

$$\begin{aligned}\frac{dE}{dz} &= 2B_{F_m} + 2\int_0^\infty \overline{u'v'}\frac{\partial \overline{u}}{\partial r} r dr - 2\int_0^\infty \overline{u}\frac{\partial(\overline{u'^2} - \overline{v'^2})}{\partial z} r dr \\ &= 2B_{F_m} + 2\frac{B_{F_m} I_4}{I_6} - J,\end{aligned} \tag{42}$$

where $E = 2\pi\int_0^\infty \overline{u}^3 r dr$, so that $E/2$ is the flux of mean kinetic energy and $J = 2\int_0^\infty \overline{u}\frac{\partial(\overline{u'^2}-\overline{v'^2})}{\partial z} r dr$. Here $I_4 = 2\pi\int_0^\infty f_1' f_4 \tau d\tau$ and $I_6 = 2\pi\int_0^\infty f_1 f_3 \tau d\tau$. Now using Eqs. (42) and (6b), we have

$$\frac{dQ}{dz} = 2\left(\frac{\mathrm{Ri}}{\mathcal{B}}(\mathcal{A}-1) - \frac{QB_{F_m}}{EM^{1/2}}\frac{I_4}{I_6} + \frac{Q}{2EM^{1/2}}J + \frac{Q}{2M^{1/2}}\frac{d\ln\mathcal{B}}{dz}\right)M^{1/2}, \tag{43}$$

where $\mathcal{A} = \frac{E}{B_{F_m}M}\frac{dM}{dz} = I_3 I_5/I_6(I_2 + I_f)$ with $I_3 = 2\pi\int_0^\infty f_1^3 \tau d\tau$ and $I_5 = 2\pi\int_0^\infty f_3 \tau d\tau$, $\mathcal{B} = QE/M^2 = I_1 I_3/(I_2 + I_f)^2$, and $\mathrm{Ri} = \frac{B_{F_m}Q^2}{M^{5/2}} \propto d\delta(z)/dz$. Since here self-preserving solutions are obtained by neglecting the terms containing $(\overline{u'^2} - \overline{v'^2})$ and $\overline{u'\theta'}$ in the mean equations, therefore, here $I_f = 0$, $B_{F_f} = 0$, and $J = 0$. This implies that $B_F = B_{F_m}$, and $M = M_m$. Also, note that Shabbir and George [2] suggested to ignore the integral I_f in analysis of axisymmetric plume as they found its contribution to the kinematic momentum flux very small. Since $\mathcal{B}$ is a constant in z, therefore $\frac{d\ln\mathcal{B}}{dz} = 0$. Therefore, we have

$$\frac{dQ}{dz} = 2\frac{\mathrm{Ri}}{\mathcal{B}}(\mathcal{A} - 1 + \mathcal{C})M^{1/2}, \tag{44}$$

where $\mathcal{A}$, $\mathcal{B}$, $\mathcal{C}$, and Ri are given by

$$\mathcal{A} = \frac{I_3 I_5}{I_6 I_2},\ \mathcal{B} = \frac{I_1 I_3}{I_2^2}, \mathcal{C} = -\frac{I_4}{I_6}, \quad \text{and} \quad \mathrm{Ri} = \mathrm{Ri}_c\left[\frac{(z+a)}{z_0}\right]^{-1+a_2/a_1}, \quad \text{with } \mathrm{Ri}_c = \frac{I_6 I_1^2}{I_2^{5/2}}. \tag{45}$$

Now comparing the above equation with Eq. (41), we found the entrainment coefficient α as

$$\begin{aligned}\alpha &= \frac{\mathrm{Ri}}{\mathcal{B}}(\mathcal{A} - 1 + \mathcal{C}) \\ &= \alpha_c\left[\frac{(z+a)}{z_0}\right]^{-1+a_2/a_1},\ a_1 \neq 0.\end{aligned} \tag{46}$$

Here the coefficient α_c is given by

$$\alpha_c = \frac{\mathrm{Ri_c}}{\mathcal{B}}(\mathcal{A} - 1 + \mathcal{C}) = \frac{I_1}{\sqrt{I_2}}\left[\frac{I_5}{I_2} - \frac{(I_4 + I_6)}{I_3}\right]. \tag{47}$$

For the above expression, the value of α_c depends on the radial profiles of vertical (axial) velocity, temperature difference, and Reynolds shear stress. We found that $\frac{I_5}{I_2} - \frac{(I_4+I_6)}{I_3}$ is fixed for each

TABLE II. Values of the coefficients $\mathcal{A}$, $\mathcal{B}$, and Ri_c in Eq. (45) and $\mathcal{C}$, α_c, and α_{Gc}.

	$\mathcal{A}$	$\mathcal{B}$	$\mathcal{C}$	Ri_c	α_c	α_{Gc}
Rouse *et al.* [6]						0.08552
Papanicolaou and List [12]						0.0875
George *et al.* [11]						0.107583
Yannopoulos [41] (FOA Solns.)						0.10
SOA Solns.						0.0917
Present theory:						
$\gamma = 0.0165$						
$m = 0$ $(a_2/a_1 = 1, \sigma_t = 1.1)$	1.2	1.8	0.55	1.05735	0.440561	0.115585
$m = 1/2$ $(a_2/a_1 = 5/7, \sigma_t = 1.05556)$	1.2	1.8	0.475	1.09269	0.409758	0.107503
$m = 4/5$ $(a_2/a_1 = 11/19, \sigma_t = 1.02381)$	1.2	1.8	0.43	1.12994	0.395481	0.103757
$m = 1$ $(a_2/a_1 = 1/2, \sigma_t = 1)$	1.2	1.8	0.4	1.16272	0.387574	0.101683

value of the ratio a_2/a_1 as it is equal to $(1/6)(1 + 4a_2/a_1)$ independent of γ. Thus, we can also write $\alpha_c = (1/6)(1 + 4a_2/a_1)I_1/\sqrt{I_2}$. Therefore, when $a_1 = a_2$, then $\alpha_c = (5/6)I_1/\sqrt{I_2}$, while for $a_2/a_1 = 1/2$, $\alpha_c = I_1/(2\sqrt{I_2})$. A value of γ as discussed in the previous section can be estimated for comparison of the profile functions obtained here with experimental measurements and hence a value of α_c can be obtained. However, the value of γ estimated from the available experiments of axisymmetric plume can give only the value of entrainment coefficient for $a_2/a_1 = 1$ which corresponds to $m = 0$ (Kolmogorov equilibrium dissipation), and further experimental measurements similar to planar jets and axisymmetric wake measurements in Refs. [22,26] are required to obtain coefficient values α and α_c precisely in the non-Kolmogorov dissipation regime with $m = 1$ of axisymmetric plume. The value of $\alpha(= \alpha_c)$ when $a_2/a_1 = 1$ $(m = 0)$ and $\gamma = 0.0165$ for the solutions Eq. (32) with Eqs. (33) and (34) of the axisymmetric plume in unstratified ambient is obtained as 0.440561, which remains constant with the increase in vertical height of the plume. We can write Eq. (44) as

$$\frac{d\overline{u}_c\delta_{u/e}^2}{dz} = 2\alpha_G\delta_{u/e}\overline{u}_c, \tag{48}$$

where $\alpha_G = \alpha\delta_{u/e}\sqrt{I_2}/I_1$. We can write $\alpha_G = \alpha_{Gc}(z + a/z_0)^{(-1+a_2/a_1)}$, where $\alpha_{Gc} = \alpha_c b_{u/e}\sqrt{I_2}/I_1 = (1/6)(1 + 4a_2/a_1)b_{u/e}$, $a_1 \neq 0$. A comparison of α_{Gc} with some experimental values is given in Table II. Table II also contains the values of the parameters $\mathcal{A}$, $\mathcal{B}$, $\mathcal{C}$, Ri_c, and α_c. Note that the value of $\mathcal{A}$ and $\mathcal{B}$ are fixed as the ratio a_2/a_1 of group parameters is varied. We can see that the obtained value of α_{Gc} when $a_1 = a_2(m = 0)$ lies within the range 0.07–0.16 of entrainment coefficient obtained by various experimental measurements. When $m = 1$, here the entrainment coefficient decreases as $\alpha \propto (z + a)^{-1/2}$, while in planar plume $\alpha \propto (z + a)^{-3/5}$ and so decays faster than the axisymmetric plume. This difference is mainly due to the difference in source configuration of the two plumes. The values of the coefficients α_c and α_{Gc} change with a change in the value of γ, which is arbitrary and depends on source conditions. Note that if $a_1 = 0$ but $a_0 \neq 0$ and $a_2 \neq 0$, then $\alpha = \alpha_c \mathrm{Exp}[a_2 z/a_0 z_0]$ with α_c is as defined by Eq. (47). We found that $d\delta(z)/dz$ can be written as

$$\frac{d\delta}{dz} = \frac{\sqrt{I_2}}{I_1}\left(2\alpha - \frac{\mathrm{Ri}}{2}\frac{\mathcal{A}}{\mathcal{B}}\right). \tag{49}$$

Using Eq. (46), we can write

$$\frac{d\delta}{dz} = \alpha\frac{\sqrt{I_2}}{I_1}\left[2 - \frac{\mathcal{A}}{2(\mathcal{A} - 1 + \mathcal{C})}\right], \tag{50}$$

or

$$\frac{d\delta}{dz} = \frac{\mathrm{Ri}}{\mathcal{B}}\left(\frac{3}{2}\mathcal{A} - 2 + 2\mathcal{C}\right)\frac{\sqrt{I_2}}{I_1}. \tag{51}$$

The dissipation coefficient in general is directly proportional to the rate of spreading of plume velocity/temperature difference width, i.e., $C_{\epsilon_u} \propto d\delta_{u/n}/dz$. Again $d\delta_{u/n}/dz = b_{u/n} d\delta(z)/dz$ and $d\delta_{\theta/n}/dz = b_{\theta/n} d\delta(z)/dz$, so here from Eqs. (50) and (51) we can say the plume velocity and temperature spreading rates are related directly to the entrainment coefficient α (or α_G) and local Richardson number Ri. Therefore, we can write

$$C_{\epsilon_u} \propto b_{u/n}\, \alpha \frac{3\mathcal{A} + 4\mathcal{C} - 4}{2(\mathcal{A} + \mathcal{C} - 1)}\frac{\sqrt{I_2}}{I_1}, \tag{52}$$

or

$$C_{\epsilon_u} \propto b_{u/n} \frac{\mathrm{Ri}}{\mathcal{B}}\left(\frac{3}{2}\mathcal{A} - 2 + 2\mathcal{C}\right)\frac{\sqrt{I_2}}{I_1}. \tag{53}$$

Note that $C_{\epsilon_u} \propto C_{\epsilon_\theta} \propto C_\epsilon$. This establishes the well-known result from previous analysis that dissipation coefficients ($C_\epsilon, C_{\epsilon_u}, C_{\epsilon_\theta}$) depend on entrainment coefficient. The relations Eqs. (52) and (53), respectively, between dissipation coefficient and entrainment coefficient and local Richardson number are universal, that is, the relations hold irrespective of whether the turbulence dissipation is Kolmogorov or non-Kolmogorov. Note that the entrainment coefficient is not uniform and differs under changing circumstances. It is obvious that turbulent energy dissipation would change if entrainment coefficient changes under differing conditions. So, for non-Kolmogorov dissipation the entrainment coefficient instead of being a constant varies with streamwise distance as a power law. The power exponent varies as the value of m varies in (0,1]. This is evident in the foregoing discussion.

Note that Cafiero and Vassilicos [22] have observed this sort of scaling for entrainment coefficient in planar jet. They found that in the planar jet, entrainment coefficient in a non-Kolmogorov region with $m = 1$ decreases as $-1/3$ power of streamwise distance. The same result was also established theoretically by Layek and Sunita [21] in planar jet. The link between entrainment and dissipation is well known in Kolmogorov dissipation region.

Here we can conclude that the dissipation and entrainment coefficient are related in general. When dissipation is Kolmogorov ($m = 0$, $a_2/a_1 = 1$) then entrainment coefficient is a constant, while when the dissipation is non-Kolmogorov ($m \neq 0$, $a_2/a_1 \neq 1$) the entrainment coefficient varies with axial distance. The above analysis clearly indicates the importance of the ratio a_2/a_1 of the two stretching group parameters that determines the existence of non-Kolmogorov nonequilibrium and Kolmogorov equilibrium dissipations. In other words, relationship between Kolmogorov dissipation and self-similarity is explored through the value of the ratio a_2/a_1. Thus, the question arises how the transition occurs from $a_2/a_1 \neq 1$ to $a_2/a_1 = 1$. In grid generated decaying turbulence it was shown that the nonequilibrium dissipation region is switched over a classical dissipation region abruptly further downstream distance. This suggests that the transition from nonequilibrium to equilibrium is caused by a sudden breaking of large scale coherent structures formed due to the engulfment process of entrainment vortex motion of this boundary-free shear flow. There need further research works on the fundamental mechanism of turbulence cascade in the depletion of non-Kolmogorov TKE dissipation and eventually enters the Kolmogorov equilibrium dissipation region.

VI. CONCLUSIONS

A detailed symmetry analysis for mean equations along with the Reynolds stress model to the boundary layer flow of an axisymmetric turbulent plume in an unstratified environment is presented, which garner unconventional and novel scalings of individual components of flow quantities in plume. The implications of nonequilibrium dissipation are discussed and quantified in comparison to classical scaling laws, which are compared with existing data. The new dissipation laws connected with entrainment coefficient are found, which obey the linear proportionality to the plume spreading rate and are non-Kolmogorov when spreading rate is nonconstant. The symmetry-based eddy viscosity closure model, which although not work very well at the plume edges is designed relevant to the present study. Entrainment coefficient is at odds with the classical studies when non-Kolmogorov dissipation holds but its trend is in agreement with recent experimental and theoretical studies for planar jet. It has been shown that how two geometric stretching parameters determine the existence of Kolmogorov and non-Kolmogorov dissipation laws. This work explores four important results, which are summarized below:

(i) The dissipations laws occur with dissipation coefficient C_ϵ evolving linearly with spreading rates $d\delta/dz$ of plume. A particular case is identified in which the spreading rates can be expressed in terms of mth power of the ratio of global constant Reynolds number to the local Reynolds number varying with the streamwise distance, where $m = 3(a_1 - a_2)/(a_1 + a_2)$, $a_1 \neq -a_2$. So, $C_\epsilon \propto d\delta/dz \propto (\mathrm{Re}_G/\mathrm{Re}_\delta)^m$. It indicates a dependence of dissipation laws on local Reynolds number in the region where $m \neq 0$. This is at odds with constant dissipation coefficient of Kolmogorov universal law, which holds only when the stretching parameters a_1 and a_2 collapse into one, that is, when $a_1 = a_2$ and the value of $m = 0$. So, the relation between complete self-similarity and Kolmogorov laws is established in this study through the two stretching group parameters. On contrary, non-Kolmogorov laws correspond to incomplete similarity or partial self-preservation in plume.

(ii) The present theoretical analysis showed different power-law evolutions of components of flow quantities, in particular, Reynolds stress tensor, pressure-strain-rate tensor, and dissipation tensor. The pressure-strain-rate relation (sum of the three pressure-strain-rate components equated to zero) is not similar. This occurs when $m \neq 0$ implying nonequality of the stretching parameters a_1 and a_2. As a consequence it gives nonconstant spreading rate and new dissipation laws in contrast to constant spreading rate of Kolmogorov theory.

(iii) The well-known link between entrainment and dissipation is revisited in the non-Kolmogorov turbulence. It is established that turbulent dissipation depends on entrainment coefficient in the non-Kolmogorov region. Entrainment coefficient is directly proportional to the spreading rates and hence is proportional to dissipation coefficient when non-Kolmogorov dissipation holds. The constant of proportionality depends mainly on integrals of mean axial velocity up to order three, mean temperature difference, and turbulent stresses. This implies that entrainment process and turbulent dissipation are related in general irrespective of whether the dissipation is Kolmogorov or non-Kolmogorov. The entrainment coefficient decays with the vertical rise of the plume in the region of non-Kolmogorov dissipation depending upon the ratio of symmetry group parameters $a_2/a_1(> 0)$ which support the experimental visualization of entrainment in planar jet flow. The entrainment coefficient is directly proportional to the local Richardson number, which also varies with the height of the plume. It is found that the entrainment coefficient decays slowly with power-law exponent $-1/2$ in axisymmetric plume than the planar plume in which the power-law exponent is $-3/5$ when $m = 1$.

(iv) It is revealed that the two stretching group parameters a_1 and a_2 emerged from symmetry analysis of the model equations of plume, are involved in the evolution and determination of the occurrence of the Kolmogorov and non-Kolmogorov dissipation laws. It is found that for Kolmogorov dissipation theory the statistical equations are form invariant under one translation and one stretching transformation. For non-Kolmogorov theory, the stretching group parameters are not equal and their ratio can take multiple values but is uniquely determined. Results are agreed with experimental data and explained physically, in particular, the theoretical prediction of spreading rate for non-Kolmogorov dissipations is agreed with the flow visualization in jet where local Reynolds number is increasing.

Thus, the present study focuses the impact of non-Kolmogorov dissipation on scaling laws for turbulent buoyant plumes. It generalizes the dissipation theory and also showed its dependence on varying spreading rate or entrainment coefficient and hence on mean flow parameters. The analysis reveals that pressure-strain-rate terms introduce pressure forces resulting in partial self-preservation for a significant range and the non-Kolmogorov dissipation exists in plume. Moreover, the dissipation of thermal fluctuation follows non-Kolmogorov law when dissipations of Reynolds stress tensor and TKE are non-Kolmogorov (nonequilibrium), which is consistent with the work of Layek and Sunita [19] and the premonition of Lumley [31].

ACKNOWLEDGMENTS

We thank the referees for their valuable comments, which helped a lot to improve the manuscript. This work was partially supported by DST-FIST Programme, New Delhi, India [No. SR/FST/MSII/2017/10(C)]. Prof. G. C. Layek thanks Prof. J. C. Vassilicos for participating in discussions on non-Kolmogorov turbulent plume flows during his visit as Professeur invité at LMFL-Laboratoire de Mécanique des fluides de Lille-Kampé de Fériet, F-59000 Lille, France.

APPENDIX

In the present study we used Lie symmetry group theory for symmetry analysis of turbulent round plume. See Ref. [42] and the Appendix of Refs. [19,21,25] and the books Cantwell [32] and Layek [43] for the basics of Lie group theory. Since the number of equations and variables are large, so here we used the Mathematica software package introtosymmetry.m by Cantwell [32] for the symmetry analysis. Here we write the simplified infinitesimal transformations ξ_z, ξ_r, $\eta_{\overline{u}}$, $\eta_{\overline{v}}$, η_θ, $\eta_{\overline{u'v'}}$, $\eta_{\overline{u'^2}}$, and $\eta_{\overline{\theta'^2}/2}$ of z, r, $\overline{u}$, $\overline{v}$, θ, $\overline{u'v'}$, $\overline{u'^2}$, and $\overline{\theta'^2}/2$, respectively, as follows:

$$\xi_z = a_0 + a_1 z,\ \xi_r = a_2 r,\ \eta_{\overline{u}} = (a_1 - 2a_2)\overline{u}/3\eta_{\overline{v}} = (-2a_1 + a_2)\overline{v}/3,\ \eta_\theta = -(a_1 + 4a_2)\theta/3,$$
$$\eta_{\overline{u'v'}} = -(a_1 + a_2)\overline{u'v'}/3,\ \eta_{\overline{u'^2}} = (2a_1 - 4a_2)\overline{u'^2}/3,\ \eta_{\overline{\theta'^2}} = -2(a_1 + 4a_2)\overline{\theta'^2}/3. \quad \text{(A1)}$$

Thus, the equations remain form invariant under one translation group (G_{a_0}) with parameter a_0 and two stretching transformations (G_{a_1} and G_{a_2}) with group parameters a_1 and a_2 and are given by

$$G_{a_0}: \widetilde{z} = z + a_0, \widetilde{r} = r, \widetilde{\overline{u}} = \overline{u}, \widetilde{\overline{v}} = \overline{v}, \widetilde{\theta} = \theta, \widetilde{\overline{u'v'}} = \overline{u'v'}, \widetilde{\overline{v'\theta'}} = \overline{v'\theta'}, \widetilde{\overline{u'\theta'}} = \overline{u'\theta'}, \widetilde{\overline{u'^2}} = \overline{u'^2}, \widetilde{\overline{v'^2}} = \overline{v'^2},$$
$$\widetilde{\overline{w'^2}} = \overline{w'^2}, \widetilde{\overline{k_\theta}} = \overline{k_\theta}, \widetilde{(\overline{u'^2} - \overline{v'^2})} = (\overline{u'^2} - \overline{v'^2}), \widetilde{\epsilon_u} = \epsilon_u, \widetilde{\epsilon_v} = \epsilon_v, \widetilde{\epsilon_w} = \epsilon_w, \widetilde{\epsilon_\theta} = \epsilon_\theta. \quad \text{(A2a)}$$

$$G_{a_1}: \widetilde{z} = z\mathrm{e}^{a_1}, \widetilde{r} = r, \widetilde{\overline{u}} = \mathrm{e}^{a_1/3}\overline{u}, \widetilde{\overline{v}} = \mathrm{e}^{-2a_1/3}\overline{v},$$
$$\widetilde{\theta} = \mathrm{e}^{-a_1/3}\theta, \widetilde{\overline{u'v'}} = \mathrm{e}^{-a_1/3}\overline{u'v'}, \widetilde{\overline{v'\theta'}} = \mathrm{e}^{-a_1}\overline{v'\theta'},$$
$$\widetilde{\overline{u'\theta'}} = \overline{u'\theta'}, \widetilde{\overline{u'^2}} = \mathrm{e}^{2a_1/3}\overline{u'^2}, \widetilde{\overline{v'^2}} = \mathrm{e}^{-4a_1/3}\overline{v'^2}, \widetilde{\overline{w'^2}} = \mathrm{e}^{-4a_1/3}\overline{w'^2}, \widetilde{\overline{k_\theta}} = \mathrm{e}^{-2a_1/3}\overline{k_\theta},$$
$$\widetilde{(\overline{u'^2} - \overline{v'^2})} = \mathrm{e}^{2a_1/3}(\overline{u'^2} - \overline{v'^2}), \widetilde{\epsilon_u} = \epsilon_u, \widetilde{\epsilon_v} = \mathrm{e}^{-2a_1}\epsilon_v,$$
$$\widetilde{\epsilon_w} = \mathrm{e}^{-2a_1}\epsilon_w, \widetilde{\epsilon_\theta} = \mathrm{e}^{-4a_1/3}\epsilon_\theta. \quad \text{(A2b)}$$

$$G_{a_2}: \widetilde{z} = z, \widetilde{r} = \mathrm{e}^{a_2}r, \widetilde{\overline{u}} = \mathrm{e}^{-2a_2/3}\overline{u}, \widetilde{\overline{v}} = \mathrm{e}^{a_2/3}\overline{v},$$
$$\widetilde{\theta} = \mathrm{e}^{-4a_2/3}\theta, \widetilde{\overline{u'v'}} = \mathrm{e}^{-a_2/3}\overline{u'v'}, \widetilde{\overline{v'\theta'}} = \mathrm{e}^{-a_2}\overline{v'\theta'},$$
$$\widetilde{\overline{u'\theta'}} = \mathrm{e}^{-2a_2}\overline{u'\theta'}, \widetilde{\overline{u'^2}} = \mathrm{e}^{-4a_2/3}\overline{u'^2}, \widetilde{\overline{v'^2}} = \mathrm{e}^{2a_2/3}\overline{v'^2}, \widetilde{\overline{w'^2}} = \mathrm{e}^{2a_2/3}\overline{w'^2}, \widetilde{\overline{k_\theta}} = \mathrm{e}^{-8a_2/3}\overline{k_\theta},$$
$$\widetilde{(\overline{u'^2} - \overline{v'^2})} = \mathrm{e}^{-4a_2/3}(\overline{u'^2} - \overline{v'^2}), \widetilde{\epsilon_u} = \mathrm{e}^{-2a_2}\epsilon_u, \widetilde{\epsilon_v} = \epsilon_v, \widetilde{\epsilon_w} = \epsilon_w, \widetilde{\epsilon_\theta} = \mathrm{e}^{-10a_2/3}\epsilon_\theta. \quad \text{(A2c)}$$

Note that the infinitesimals forms of Eq. (A1) can be obtained by the Taylor series expansions of the transformations Eqs. (A2a), (A2b), and (A2c) about the symmetry group parameters $\varepsilon = 0$, where $\varepsilon \equiv (a_0, a_1, a_2)$ and then neglecting the terms containing second and higher orders of ε.

The infinitesimals ξ_i and η_U (written after adding the infinitesimals for each parameter) then forms a characteristic system using the Lie invariance principle and invariance surface condition (see the Appendix of Refs. [19,21] and the book in Ref. [32]). Solving the characteristic system, the invariant solutions are obtained.

---

[1] G. K. Batchelor, Heat convection and buoyancy effects in fluids, Q. J. R. Meteorol. Soc. **80**, 339 (1954).
[2] A. Shabbir and W. K. George, Experiments on a round turbulent buoyant plume, J. Fluid Mech. **275**, 1 (1994).
[3] B. R. Ramaprian and M. S. Chandrasekhara, Measurements in vertical plane turbulent plumes, J. Fluids Eng. **111**, 69 (1989).
[4] Y. B. Zel'dovich, The asymptotic laws of freely-ascending convective flows, Zh. Eksp. Teor. Fiz. **7**, 1463 (1937) (in Russian). English transl. in *Selected Works of Yakov Borisovich Zeldovich*, edited by J. P. Ostriker (Princeton University Press, Princeton, NJ, 1992), Vol. 1, pp. 82–85.
[5] W. Schmidt, Turbulent propagation of a stream of air, Angew. Math. Mech. **21**, 265 (1941).
[6] H. Rouse, C. S. Yih, and H. W. Humphreys, Gravitational convection from a boundary source, Tellus **4**, 201 (1952).
[7] C.-S. Yih, Turbulent buoyant plumes, Phys. Fluids **20**, 1234 (1977).
[8] W. K. George, The self-preservation of turbulent flows and its relation to initial conditions and coherent structures, in *Advances in Turbulence*, edited by W. K. George and R. E. A. Arndt (Hemisphere, New York, 1989), pp. 39–73.
[9] W. K. George, Some new ideas for similarity of turbulent shear flows, in *Proceedings of the ICHMT Symposium on Turbulence, Heat and Mass Transfer, Lisbon, Portugal 1994*, edited by K. Hanjalic and J. C. F. Pereira (Begell House, New York, 1995).
[10] A. Ezzamel, P. Salizzoni, and G. R. Hunt, Dynamical variability of axisymmetric buoyant plumes, J. Fluid Mech. **765**, 576 (2015).
[11] W. K. George, R. L. Alpert, and F. Tamanini, Turbulent measurements in an axisymmetric buoyant plume, Int. J. Heat Mass Tranfer **20**, 1145 (1977).
[12] P. N. Papanicolaou and E. J. List, Investigations of round vertical turbulent buoyant jets, J. Fluid Mech. **195**, 341 (1988).
[13] A. A. Townsend, *The Structure of Turbulent Shear Flow*, 2nd ed. (Cambridge University Press, Cambridge, 1976).
[14] E. Kaminski, S. Tait, and G. Carazzo, Turbulent entrainment in jets with arbitrary buoyancy, J. Fluid Mech. **526**, 361 (2005).
[15] G. Taylor, Dynamics of a mass of hot gas rising in air, U.S. Atomic Energy Commission MDDC 919, LADC 276 (1945).
[16] B. R. Morton, G. Taylor, and J. S. Turner, Turbulent gravitational convection from maintained and instantaneous sources, Proc. R. Soc. London A **234**, 1 (1956).
[17] S. Paillat and E. Kaminski, Entrainment in plane turbulent pure plumes, J. Fluid Mech. **755**, R2 (2014).
[18] M. Reeuwijk and J. Craske, Energy-consistent entrainment relations for jets and plumes, J. Fluid Mech. **782**, 333 (2015).
[19] G. C. Layek and Sunita, Non-Kolmogorov scaling and dissipation laws in planar turbulent plume, Phys. Fluids **30**, 115105 (2018).
[20] G. F. Lane-Serff, Investigation of the fractal structure of jets and plumes, J. Fluid Mech. **249**, 521 (1993).
[21] G. C. Layek and Sunita, Non-Kolmogorov dissipation in a turbulent planar jet, Phys. Rev. Fluids **3**, 124605 (2018).
[22] G. Cafiero and J. C. Vassilicos, Nonequilibrium turbulence scalings and self-similarity in turbulent planar jets, Proc. R. Soc. London A **475**, 20190038 (2019).
[23] N. E. Kotsovinos, A note on the spreading rate and virtual origin of a plane turbulent jet, J. Fluid Mech. **77**, 305 (1976).

[24] P. Bradshaw, Effect of external disturbances on the spreading rate of a plane turbulent jet, J. Fluid Mech. **80**, 795 (1977).
[25] G. C. Layek and Sunita, Multitude scaling laws in axisymmetric turbulent wake, Phys. Fluids **30**, 035101 (2018).
[26] J. Nedić, J. C. Vassilicos, and B. Ganapathisubramani, Axisymmetric Turbulent Wakes with New Nonequilibrium Similarity Scalings, Phys. Rev. Lett. **111**, 144503 (2013).
[27] T. Dairay, M. Obligado, and J. C. Vassilicos, Nonequilibrium scaling laws in axisymmetric turbulent wakes, J. Fluid Mech. **781**, 166 (2015).
[28] A. Thormann and C. Meneveau, Decay of homogeneous, nearly isotropic turbulence behind active fractal grids, Phys. Fluids **26**, 025112 (2014).
[29] S. Goto and J. C. Vassilicos, Energy dissipation and flux laws for unsteady turbulence, Phys. Lett. A **379**, 1144 (2015).
[30] R. A. Antonia, B. R. Satyaprakash, and A. K. M. F. Hussain, Measurements of dissipation rate and some other characteristics of turbulent plane and circular jets, Phys. Fluids **23**, 695 (1980).
[31] J. L. Lumley, Some comments on turbulence, Phys. Fluids A **4**, 203 (1992).
[32] B. J. Cantwell, *Introduction to Symmetry Analysis* (Cambridge University Press, Cambridge, UK, 2002).
[33] H. J. Hussein, S. P. Capp, and W. K. George, Velocity measurements in a high-Reynolds number, momentum conserving, axisymmetric, turbulent jet, J. Fluid Mech. **258**, 31 (1994).
[34] P. B. V. Johansson, W. K. George, and M. J. Gourlay, Equilibrium similarity, effects of initial conditions and local Reynolds number on the axisymmetric wake, Phys. Fluids **15**, 603 (2003).
[35] G. Cafiero, M. Obligado, and J. C. Vassilicos, Length scales in turbulent free shear flows, J. Turbul. **21**, 243 (2020).
[36] H. Nakagome and M. Hirata, The structure of turbulent diffusion in an axisymmetrical thermal plume, in *Proceedings of the 1976 ICHMT Seminar on Turbulent Buoyant Convection* (Hemisphere, London, UK, 1977).
[37] H. Wang and A. W.-K. Law, Second-order integral model for a round turbulent buoyant jet, J. Fluid Mech. **459**, 397 (2002).
[38] H. C. Burridge, J. L. Partridge, and P. F. Linden, The fluxes and behaviour of plumes inferred from measurements of coherent structures within images of the bulk flow, Atmosphere-Ocean **54**, 403 (2016).
[39] E. K. G. Carazzo and S. Tait, The route to self-similarity in turbulent jets and plumes, J. Fluid Mech. **547**, 137 (2006).
[40] C. H. B. Priestley and F. K. Ball, Continuous convection from an isolated source of heat, Q. J. R. Meteorol. Soc. **81**, 144 (1955).
[41] P. C. Yannopoulos, An improved integral model for plane and round turbulent buoyant jets, J. Fluid Mech. **547**, 267 (2006).
[42] G. C. Layek and Sunita, On the nature of multitude scalings in decaying isotropic turbulence, Int. J. Non-Linear Mech. **95**, 143 (2017).
[43] G. C. Layek, *An Introduction to Dynamical Systems and Chaos* (Springer, India, 2015).